

# Synthesis and Evaluation of L-Rhamnose 1C-Phosphonates as Nucleotidyltransferase Inhibitors

Matthew W. Loranger,<sup>†</sup> Stephanie M. Forget,<sup>†</sup> Nicole E. McCormick,<sup>‡</sup> Raymond T. Syvitski,<sup>†,||</sup> and David L. Jakeman<sup>\*,†,‡</sup>

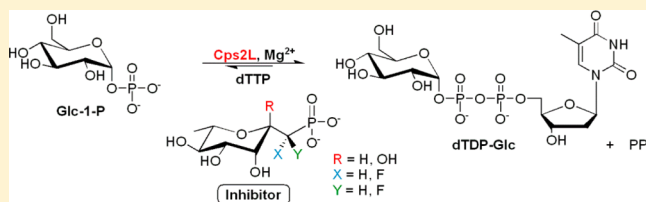
<sup>†</sup>Department of Chemistry, Dalhousie University, 6274 Coberg Road, P.O. Box 15,000, Halifax, Nova Scotia B3H 4R2, Canada

<sup>‡</sup>College of Pharmacy, Dalhousie University, 5968 College Street, P.O. Box 15,000, Halifax, Nova Scotia B3H 4R2, Canada

<sup>||</sup>National Research Council of Canada, 1411 Oxford Street, Halifax, Nova Scotia B3H 3Z1, Canada

## Supporting Information

**ABSTRACT:** We report the synthesis of a series of phosphonates and ketosephosphonates possessing an L-rhamnose scaffold with varying degrees of fluorination. These compounds were evaluated as potential inhibitors of  $\alpha$ -D-glucose 1-phosphate thymidyltransferase (Cps2L), the first enzyme in *Streptococcus pneumoniae* L-rhamnose biosynthesis, and a novel antibiotic target. Enzyme–substrate and enzyme–inhibitor binding experiments were performed using water-ligand observed binding via gradient spectroscopy (WaterLOGSY) NMR for known sugar nucleotide substrates and selected phosphonate analogues. IC<sub>50</sub> values were measured and K<sub>i</sub> values were calculated for inhibitors. New insights were gained into the binding promiscuity of enzymes within the prokaryotic L-rhamnose biosynthetic pathway (Cps2L, RmlB–D) and into the mechanism of inhibition for the most potent inhibitor in the series, L-rhamnose 1C-phosphonate.



## INTRODUCTION

*Streptococcus pneumoniae* is a prevalent, highly infectious, Gram-positive pathogen that has shown high clinical resistance to penicillin and chloramphenicol.<sup>1</sup> The mechanisms of resistance for *S. pneumoniae* and other more invasive pathogens, including *Mycobacterium tuberculosis*, usually entail alterations to drug target proteins involved in cell wall synthesis.<sup>2–5</sup> Bacterial chemo-resistance, including resistance to synergistic treatments using  $\beta$ -lactams and aminoglycosides, is a growing barrier to the treatment of invasive pathogens (i.e., *S. pneumoniae* and *M. tuberculosis*).<sup>6</sup>

Cell wall biosynthesis is a commonly pursued target for a variety of bacterial enzyme inhibitors as cell wall assembly is essential for bacterial survival and virulence. L-Rhamnose (6-deoxy-L-mannose) serves as the linking unit between arabinogalactan and peptidoglycan<sup>7,8</sup> and is a necessary constituent of the bacterial cell wall in many bacterial species.<sup>9</sup> The biosynthesis of L-rhamnose begins with nucleotidyltransferase enzymes (Cps2L/RmlA) responsible for generating activated sugars in the form of glycosylated nucleoside diphosphates (NDPs). These NDPs are generated from the enzymatic coupling of sugar 1-phosphates with nucleoside triphosphates (NTPs). Once formed, the NDPs may be further modified by intermediate enzymes (RmlB–D) before serving as substrates for glycosyltransferases.<sup>10</sup> Sugar 1-phosphate nucleotidyltransferases are vital to most biological glycosylation systems and are often used for the chemo-enzymatic synthesis of sugar nucleotides.<sup>11</sup> Nucleotidyltransferases are an attractive antimicrobial target, in that they show broad homology across various species.<sup>12</sup>

Cps2L (EC 2.7.7.24) is a thymidyltransferase responsible for coupling  $\alpha$ -D-glucose 1-phosphate (1, Glc-1-P) and deoxythymidine triphosphate (2, dTTP) to form deoxythymidine diphosphate- $\alpha$ -D-glucose (3, dTDP-Glc) (Figure 1). RmlB (EC 4.2.1.46) is responsible for oxidation of the C4'' hydroxyl unit and C6'' dehydration. RmlC (EC 5.1.3.13) catalyzes an uncommon double-epimerization at both C3'' and C5''. Finally, RmlD (EC 1.1.1.133) implements a reduction at C4'' to produce dTDP- $\beta$ -L-rhamnose (6) (Figure 2).<sup>13</sup> dTDP- $\beta$ -L-rhamnose has been shown to act as an allosteric inhibitor of the thymidyltransferase in the

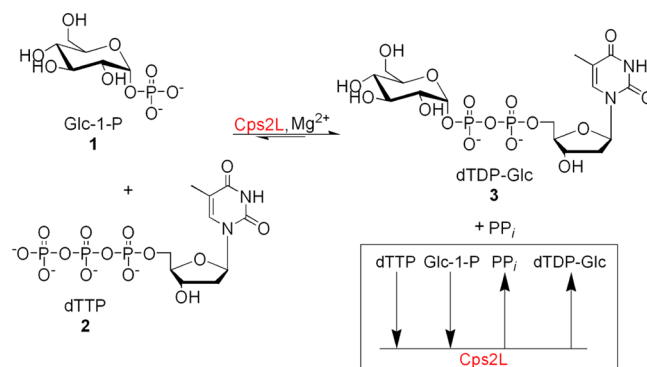


**Figure 1.** Physiological reaction catalyzed by Cps2L and ordered Bi–Bi mechanism (inset).

Received: July 17, 2013

Published: September 10, 2013

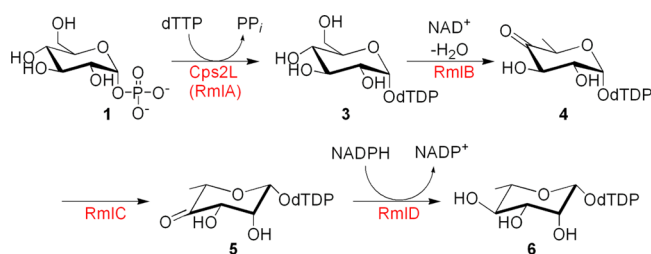


Figure 2. Reactions catalyzed by Cps2L(RmlA) and RmlB–D.

biosynthetic pathway, with the allosteric site presumed to be the point of regulatory control.<sup>9,14,15</sup> A series of thymine-based small molecule inhibitors was developed by Naismith and co-workers and was found to exhibit nanomolar inhibition against RmlA (*Pseudomonas aeruginosa*).<sup>9</sup> To date, these are the most effective reported inhibitors against nucleotidyltransferases.

Many phosphonates have biomedical applications.<sup>16,17</sup> Fosfomycin, a phosphonate containing natural product isolated from soil bacteria in 1969, has broad spectrum antibacterial activity.<sup>18</sup> Dichloromethylene diphosphonic acid (chlodronic acid) has been shown to inhibit RNA polymerase activity in influenza,<sup>19</sup> and both the related mono- and difluoromethylene diphosphonates have shown activity as bone lysis inhibitors<sup>20</sup> and antiviral agents.<sup>21,22</sup> Methylene phosphonates have been devised as nonhydrolyzable mimics of phosphates to probe a variety of biological systems.<sup>16,17</sup> Blackburn first proposed halogenation of the methylene phosphonate functionality in an effort to better mimic the properties of the natural phosphate.<sup>23</sup> Difluoromethylene phosphonates are often prepared as phosphate

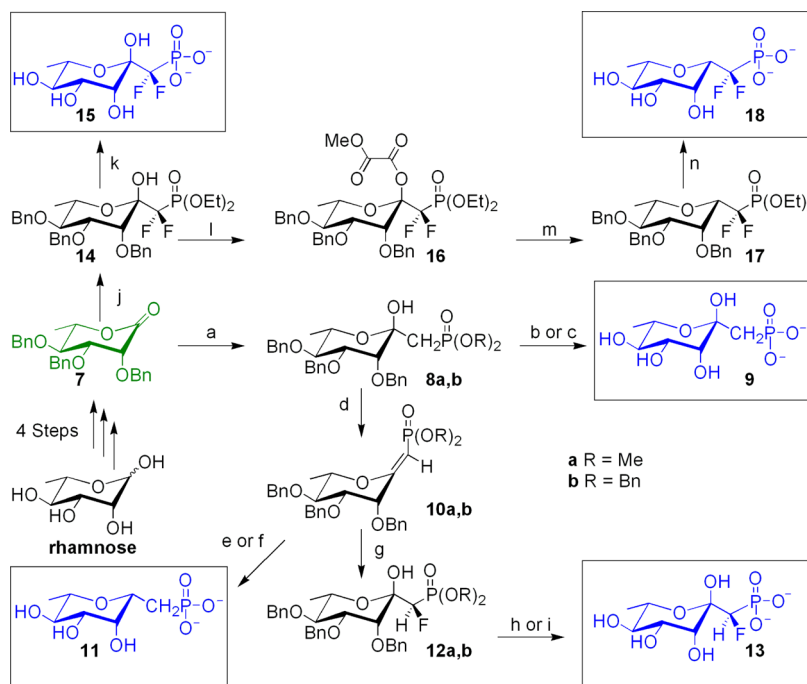
mimics due to the variety of applicable synthetic methods.<sup>17</sup> The inductive effects of two fluorine atoms results in  $pK_a$  values between 5.0 and 6.0, which are much lower than the  $pK_a$  values of physiological phosphates. The preparation of monofluoromethylene phosphonates is much less widespread, in part due to synthetic complexity.<sup>24–27</sup> The monofluoromethylene functionality ( $pK_a$  5.5–6.5<sup>27</sup>) has been shown to better mimic the electronic properties of a phosphate oxygen than the methylene unit of the phosphonate ( $pK_a$  ~7.0–8.0).<sup>17</sup> The variety of studies probing enzyme systems with substituted phosphonates demonstrates that there is no universal functionality best suited to mimic a physiological phosphate.

The design of compounds with structural scaffolds that enables them to bind multiple targets within a biosynthetic pathway would be a desirable approach to thwart rising bacterial drug resistance. Herein, we report the synthesis of a series of  $\alpha$ -L-rhamnose 1C-phosphonate compounds that utilize phosphonate and ketosephosphonate scaffolds, with varying degrees of fluorination at the C1 position, as isosteric mimics of  $\beta$ -L-rhamnose 1-phosphate. Select compounds were evaluated for binding to Cps2L and RmlB–D using water-ligand observed via gradient spectroscopy (WaterLOGSY) NMR and enzyme assay techniques

## RESULTS AND DISCUSSION

**Synthesis.** The synthesis of all analogues was initiated from lactone template 7 (Scheme 1), which was produced from commercially available  $\alpha$ -L-rhamnose following standard carbohydrate methylation, benzylation, and demethylation techniques to generate 2,3,4-tri-*O*-benzyl- $\alpha$ / $\beta$ -L-rhamnopyranose.<sup>28,29</sup>

Scheme 1. Proposed Synthesis of  $\alpha$ -L-Rhamnose Phosphonate and Ketosephosphonate Analogue Compounds<sup>a</sup>



<sup>a</sup>(a)  $\text{CH}_3\text{PO}(\text{OR})_2$ ,  $n$ -BuLi, THF,  $-78^\circ\text{C}$ , 1.5 h, R = Me (88%), R = Bn (76%); (b) (i)  $\text{H}_2$ , Pd–C, 18 h, rt, 1 psi; (ii) 6 M HCl(aq),  $100^\circ\text{C}$ , 3h; (iii)  $\text{NH}_4\text{OH}$ (aq), pH 8 (quant); (c) (i)  $\text{H}_2$ , Pd–C, 18 h, rt, 1 psi; (ii)  $\text{NH}_4\text{OH}$ (aq), pH 8 (quant); (d) MeOXCl,  $\text{CH}_2\text{Cl}_2$ , py, rt, 1.5 h, R = Me (68%), R = Bn (60%); (e) (i)  $\text{H}_2$ , Pd–C, 18 h, rt, 1 psi; (ii) 6 M HCl(aq),  $100^\circ\text{C}$ , 3h; (iii)  $\text{NH}_4\text{OH}$ (aq), pH 8 (quant); (f) (i)  $\text{H}_2$ , Pd–C, 18 h, rt, 1 psi; (ii)  $\text{NH}_4\text{OH}$ (aq), pH 8 (quant); (g) (i) Selectfluor,  $\text{CH}_3\text{CN}$ , rt, 18 h; (ii)  $\text{H}_2\text{O}$ ,  $70^\circ\text{C}$ , 2.5 h, R = Me (54%), R = Bn (22%); (h) (i)  $\text{H}_2$ , Pd–C, 18 h, rt, 1 psi; (ii) 6 M HCl(aq),  $100^\circ\text{C}$ , 3 h; (iii)  $\text{NH}_4\text{OH}$ (aq), pH 8 (quant); (i) (i)  $\text{H}_2$ , Pd–C, 18 h, rt, 1 psi (ii)  $\text{NH}_4\text{OH}$ (aq), pH 8 (quant); (j)  $\text{F}_2\text{CHPO}(\text{OEt})_2$ , LDA, THF,  $-78^\circ\text{C}$ , 0.5 h (74%); (k) (i) TMSI,  $\text{CH}_2\text{Cl}_2$ , rt, 5 h; (ii)  $\text{NH}_4\text{OH}$ (aq), pH 8 (95%); (l) MeOXCl,  $\text{CH}_2\text{Cl}_2$ , py, rt, 1.5 h (69%); (m)  $\text{Bu}_3\text{SnH}$ , AIBN, tol,  $105^\circ\text{C}$ , 1 h (85%); (n) TMSI,  $\text{CH}_2\text{Cl}_2$ , rt, 5 h, (ii)  $\text{NH}_4\text{OH}$ (aq), pH 8 (94%).

The selectively deprotected sugar was then oxidized using Albright–Goldman<sup>30</sup> conditions, in a dimethyl sulfoxide (DMSO) and acetic anhydride solvent mixture, to afford the starting material 7. Lactone 7 was transformed into the dimethyl or dibenzyl ketosephosphonate species **8a** (88% yield) and **8b** (76% yield), using lithiated salts of dimethyl methylphosphonate and dibenzyl methylphosphonate,<sup>31</sup> respectively, in tetrahydrofuran (THF) at  $-78^{\circ}\text{C}$ . Both compounds were isolated as the single axial hydroxyl isomer as determined using  $^{31}\text{P}$  and  $^1\text{H}$  NMR spectroscopy. Olefins **10a** and **10b** were produced from the in situ formation, and subsequent elimination, of the oxalyl esters formed when ketosephosphonates **8a** and **8b** were treated with methyl oxalyl chloride (MeOXCl) in a 7:2  $\text{CH}_2\text{Cl}_2$ :pyridine solvent mixture. Complete deoxygenation of the oxalyl esters was not achieved, as the reaction conditions generally produced an approximate 2:1 ratio of the desired olefin products to intermediate oxalyl esters. Previously, the use of freshly distilled pyridine or further refluxing in toluene had facilitated complete deoxygenation of related gluco-ketosephosphonate oxalyl esters.<sup>27</sup> Such measures were found to be ineffective for the L-rhamnose analogues. The intermediate oxalyl esters were always visible as the less polar species by thin layer chromatography (TLC) analysis. Olefins **10a** and **10b** were single Z stereoisomers as determined by  $^{31}\text{P}$  and  $^1\text{H}$  NMR spectroscopy, and by 1D nuclear Overhauser effect spectroscopy (NOESY) NMR experiments (Figure 3). Irradiation of the olefin proton

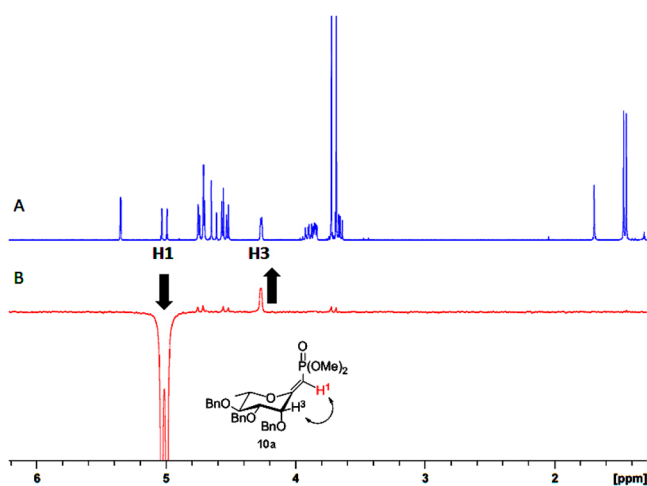


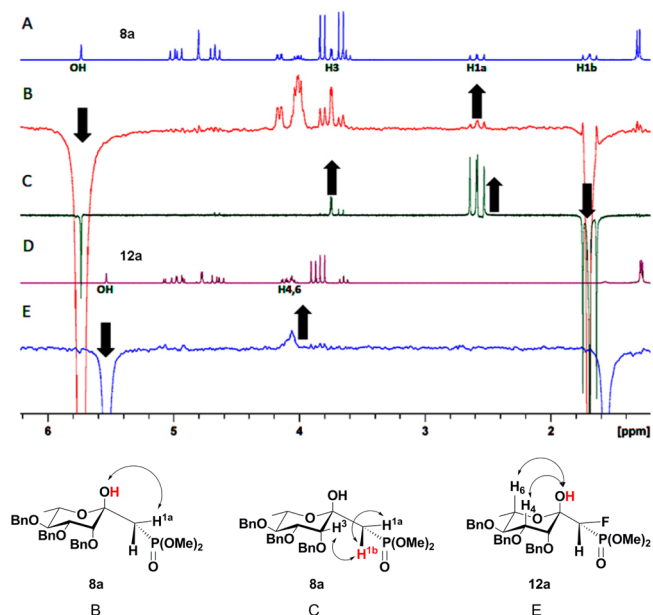
**Figure 3.**  $^1\text{H}$  NMR and 1D NOESY NMR spectra (300 MHz,  $\text{CDCl}_3$ ) for **10a**. (A)  $^1\text{H}$  NMR spectroscopy for **10a**. (B) 1D NOESY spectrum for **10a** H1. Down arrow indicates site of irradiation. Up arrow indicates a positive NOE.

H1 of compound **10a** produced an NOE at the equatorial H3 proton, suggesting a Z orientation about the double bond. If H1 had been in an E orientation, an NOE with the axial H6 and/or L-rhamnose methyl  $\text{CH}_3$  moiety would have been expected. Such effects were not observed. Determination of stereochemistry about the double bond of olefin **10a** has not been reported in its previous synthesis.<sup>32</sup>

The L-rhamnose olefins (**10a** and **10b**) were found to be significantly more prone to  $\text{C}=\text{C}$  hydration than the analogous D-glucose compounds.<sup>27</sup> If left open to atmosphere or in  $\text{CDCl}_3$  overnight, partial reversion to ketosephosphonates **8a** and **8b** was observed by TLC analysis and  $^{31}\text{P}$  NMR spectroscopy. As a result, NMR characterization of **10a** and **10b** was carried out in  $\text{CD}_2\text{Cl}_2$ , and subsequent reactions or deprotections using **10a**

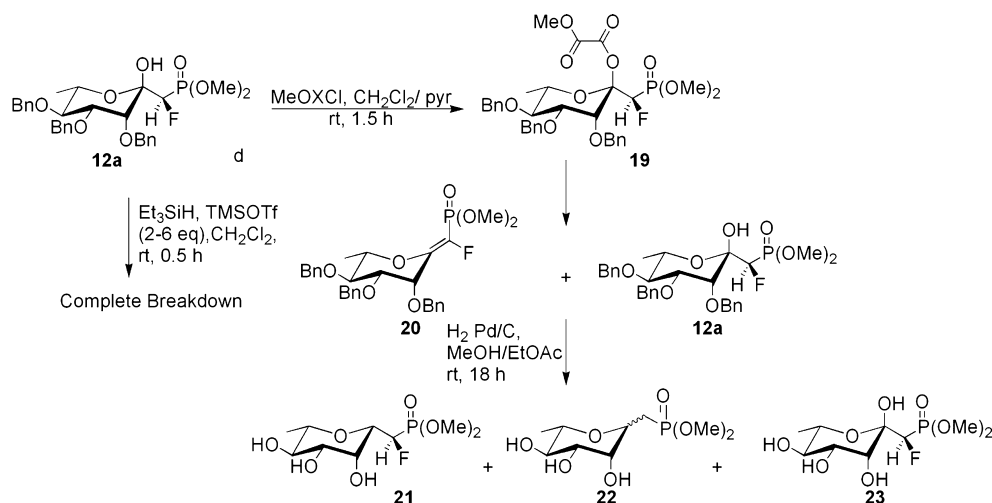
and **10b** were performed within 24 h of isolation. Treatment of **10a** or **10b** with Selectfluor<sup>33</sup> electrophilic fluorinating reagent afforded a diastereotopic mixture of monofluorinated ketosephosphonates. The major products **12a** and **12b** were isolated in 54% and 22% yields, respectively. It was suspected that the additional steric bulk of the benzyl protecting groups of **10b** reduced the fluorination efficiency, accounting for the reduced yield of **12b** relative to methyl protected **12a**.

In previous studies, direct determination of phosphonate stereochemistry for the D-glucose analogue of **12b** was possible using X-ray diffraction analysis.<sup>27</sup> In this instance, however, both the methyl (**12a**) and benzyl (**12b**) phosphonate protected L-rhamnose analogues were clear viscous liquids, rendering X-ray crystallographic techniques ineffective for stereochemical determination about the C1 position. 1D NOESY NMR experiments of compounds **8a** and **12a** were hence used to deduce the stereochemistry for compound **12a** as R. By irradiating the hydroxyl proton of **8a**, the methylene proton H1a produced an NOE (Figure 4). Irradiation of the second methylene proton H1b



**Figure 4.**  $^1\text{H}$  NMR and 1D NOESY spectra (300 MHz,  $\text{CDCl}_3$ ) for **8a** and **12a**. (A)  $^1\text{H}$  NMR spectrum for **8a**. (B) 1D NOESY spectrum for **8a** OH. (C) 1D NOESY spectrum for **8a** H1b. (D)  $^1\text{H}$  NMR spectrum for **12a**. (E) 1D NOESY spectrum for **12a** OH. Down arrow indicates site of irradiation. Up arrow indicates a positive NOE. Structure letters (B, C, and E) correspond with spectra letters. Structure bond lengths are exaggerated for clarity. Spectra B and E show artifacts resulting from trace  $\text{H}_2\text{O}$  in the samples, which should not be confused with H1b.

showed only an NOE with H1a and not the hydroxyl proton (Figure 4). It was thus reasoned that because only one of the methylene protons of **8a** showed an NOE between the hydroxyl proton and only one of the methylene protons of **8a** indicates there is no free rotation about the C1–C2 bond of the ketosephosphonates was not occurring. The subsequent 1D NOESY spectrum of **12a**, in which the hydroxyl proton was irradiated, showed that the H1a NOE had been lost, suggesting that the fluorine was occupying the H1a position at C1 (Figure 4). For **12b**, the stereochemistry was assumed to be the same as **12a**, as benzyl protecting groups on the phosphonate would be unlikely to invert the position of fluorination. Such findings were consistent with X-ray crystal structures of the analogous D-glucose

Scheme 2. Attempted Synthesis of *R* Monofluoro *L*-Rhamnose Phosphonate Analogue from Ketosephosphonate **12a**

compounds, which also showed the *R* stereoisomer to be the major product.<sup>27</sup> Nevertheless, we acknowledge that this assignment of stereochemistry is not unequivocal and necessarily relies on the equivalent dihedral angle between the PCCO bonds in compounds **8a**, **12a**, and **12b**.

Difluoro ketosephosphonate **14** was produced from the treatment of lactone **7** with diethyl difluoromethylphosphonate using lithium diisopropylamide (LDA) at  $-78\text{ }^{\circ}\text{C}$  in 74% yield. Compound **14** was converted to the corresponding oxalyl ester **16** using identical reaction conditions to those used to produce olefins **10a** and **10b**. The presence of the fluorine atoms at the C1 position renders the possibility of in situ elimination of the ester moiety unlikely, given that there are no methylene protons available for abstraction. The oxalyl ester hydrolysis product (**14**) was detected by  $^{31}\text{P}$  and  $^{19}\text{F}$  NMR spectroscopy in a minor amount (<3%) relative to the major product (**16**) after purification, indicating sensitivity of these esters to hydrolysis. Subsequent radical deoxygenation using azobisisobutyl nitrile and tributyl tin hydride in toluene, at  $105\text{ }^{\circ}\text{C}$ , afforded the difluoro phosphonate **17** in an excellent yield (85%), with a minor side product (<5%) as detected by  $^{19}\text{F}$  NMR spectroscopy. This side product is likely the axial analogue of **17** produced from in situ mutarotation of **16** under the reflux conditions required for radical deoxygenation.

Synthesis of the monofluorinated phosphonate analogue was attempted from **12a** using the oxalyl ester methodology employed for generation of the difluoro oxalyl ester analogue **16** (Scheme 2). Although complete formation of the oxalyl ester **19** was detected using TLC, standard aqueous workup or direct removal of the pyridine via concentration of the crude reaction mixture resulted in complete breakdown of the desired product into an inseparable mixture of the hydrolysis product **12a** and olefin product **20**. An alternative method of ketosephosphonate deoxygenation<sup>27</sup> starting from the monofluoro ketosephosphonate **12a** and using  $\text{Et}_3\text{SiH}$  and trimethylsilyl trifluoromethanesulfonate (TMSOTf) was explored but resulted in complete breakdown of the starting material, as was determined via TLC analysis. Attempts to perform hydrogenation on the mixture of olefin products and ketosephosphonates resulted in the production of the desired compound **21** (~40%) as well as significant amounts of the defluorinated material **22** (~20%) and the monofluoro ketosephosphonate **23** (~40%) as determined by  $^{31}\text{P}$  NMR spectroscopy. Conceivably, demethylation of the resultant mixture of phosphonates (**21–23**) and subsequent

inhibition studies on the mixture could be performed and qualitatively compared to inhibitors **9**, **11**, and **13**. Due to the complexity of the mixture of phosphonates, such additional studies were not pursued.

For the global deprotection of the methylene and monofluorinated methyl protected analogues **8a**, **10a**, and **12a**, were globally deprotected via hydrogenolysis using 20 mol %  $\text{H}_2$ -Pd/C in 1:1 MeOH/EtOAc overnight. This was followed by treatment with 6 M HCl(aq) at reflux temperatures for 3 h to cleave the phosphonate methyl esters, and subsequent titration to pH 8 with 0.2 M  $\text{NH}_4\text{OH}$ (aq) to produce the corresponding ammonium salts for enzymatic analysis. In the case of the benzyl protected analogues **8b**, **10b**, and **12b**, hydrogenolysis was performed directly followed by titration to generate the final compounds **9**, **11**, and **13**. All hydrogenation and aqueous acidic deprotection reactions produced the desired compounds in essentially quantitative yields. In the case of the difluoro analogues **14** and **17**, both benzyl and ethyl protecting groups were removed using trimethylsilyl iodide (TMSI) in  $\text{CH}_2\text{Cl}_2$ , followed by aqueous workup and titration to afford **15** and **18** in high yields (~95%) as their ammonium salts. The presence of the two fluorine atoms at C1 for the difluoro ketosephosphonate **14** seemed to stabilize the anomeric phosphonate linkage under the harsh TMSI deprotection conditions, given that attempted TMSI deprotection of the nonfluoro ketosephosphonate **8a** resulted in decomposition of the material. The increasing acidity of **9** < **13** < **15** was anticipated to correlate to a greater preference for the cyclic ( $\alpha$ -pyranose) form of the ketose. However, the ratios between the  $\alpha$ ,  $\beta$ , and open chain species were 18:2.5:1 (**9**), 100%  $\alpha$  (**13**), and 11:3:1 (**15**) as determined by  $^{31}\text{P}$  and  $^{19}\text{F}$  NMR spectroscopy (Figure 5). This remains contrary to previous studies on analogous gluco-ketosephosphonates in which the difluoro analogue was found to exist solely in the  $\alpha$ -pyranose form. Herein, the monofluoro analogue was found to be the only exclusive  $\alpha$ -pyranose *L*-rhamnose ketosephosphonate. In the case of the difluoro ketosephosphonate **15**,  $^{19}\text{F}$  NMR spectroscopy was used to determine the relative ratios of the various tautomers, due to signal overlap in the  $^{31}\text{P}$  NMR spectrum. The diastereotopic fluorine atoms appeared as AB quartets in the  $\alpha$  and the  $\beta$  pyranose forms of **15**, and appeared as a sole 2F doublet in the open chain form.

**NMR Binding Studies.** Enzyme inhibitor binding experiments were performed (a) to investigate the binding of



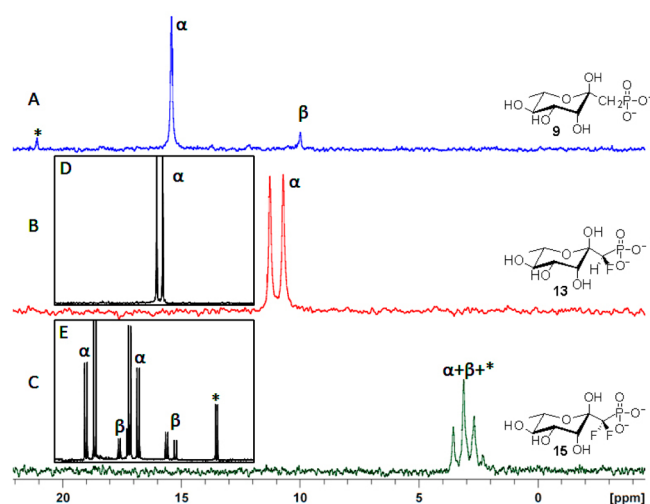


**Figure 5.**  $^{31}\text{P}$  and  $^{19}\text{F}$  (inset) NMR (300 MHz,  $\text{D}_2\text{O}$ , pH 7.5) spectra for **9**, **13**, and **15** showing ratios of  $\alpha$ : $\beta$ :open chain form (\*) of ketosephosphonates. (A) **9** 19:2.5:1. (B) **13** (100%  $\alpha$ ) verified by D ( $^{19}\text{F}$  inset). (C) **15** 11:3:1 as determined by E ( $^{19}\text{F}$  inset) due to  $^{31}\text{P}$  NMR overlap of signals.

phosphonate analogues (**9** and **11**) to enzymes (Cps2L, RmlB–D) and to gain insight into the possible mechanism of inhibition for these compounds, (b) to investigate the capacity for sugar-nucleotides dTDP-D-glucose (**3**) and dTDP-L-rhamnose (**6**) (isolated using previously established literature protocols)<sup>34</sup> to bind to multiple enzymes (Cps2L, RmlB–D) within the bacterial biosynthetic pathway, and (c) to substantiate the ordered Bi–Bi mechanism of **3** and the allosteric binding model of **6** to Cps2L. WaterLOGSY NMR was used to accomplish these goals. WaterLOGSY NMR is a 1D NOE experiment in which the irradiation of bulk water effectively facilitates magnetization transfer from active-site bound water molecules to bound ligands via the enzyme–ligand complex.<sup>35</sup> Binding compounds will maintain a perturbed magnetic state when released back into solution from the enzyme–ligand complex and produce an opposite sign NOE relative to nonbinding compounds. It is noted that with WaterLOGSY, a strong (sub nanomolar) binding interaction could result in a spectrum that appears as a nonbinding event.<sup>35</sup> This situation is not anticipated as our inhibitors are expected to be in the nanomolar to micromolar range, this situation was not anticipated. In addition, a weak or nonspecific binding event could result in the vanishing of peaks due to signal cancellation resulting from the effects of bound and unbound states.<sup>36</sup> Due to significant signal overlap within the carbohydrate region (3–4 ppm), binding events were most easily observed by the isolated L-rhamnose and/or thymidine methyl signals between 1–2 ppm.

The WaterLOGSY experiments of inhibitors **9** and **11** both showed binding to Cps2L (Figure 6). Binding was most clearly determined by the distinct methyl peak (~1.1 ppm) and methylene protons (1.5–2.5 ppm) phasing in the opposite direction to the nonbinding benzoic acid signals (7.0–8.0 ppm). Compound **11** also bound epimerase RmlC but did not appear to bind to RmlB or D (Figure 7). Competitive binding experiments were performed to see whether **11** would bind in the presence of the natural substrates Glc-1-P (**1**) or dTTP (**2**). As expected, Glc-1-P (**1**) did not bind to Cps2L in the absence of dTTP. The ordered Bi–Bi mechanism (Figure 1) of Cps2L requires binding of dTTP (**2**) to induce a conformational change

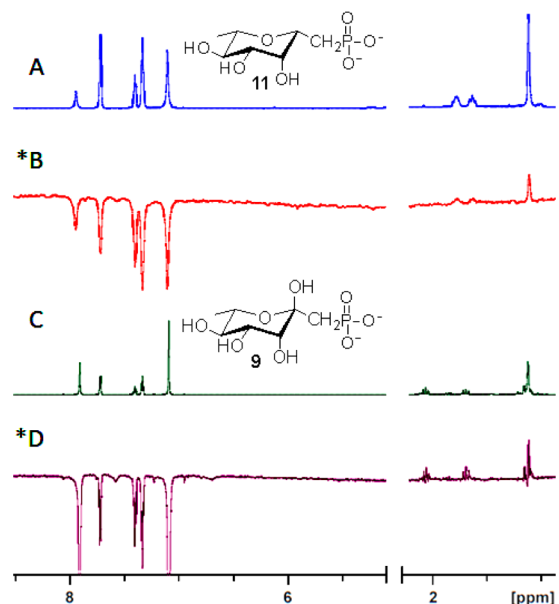


**Figure 6.** WaterLOGSY NMR spectra (700 MHz, 10:90  $\text{D}_2\text{O}/\text{H}_2\text{O}$ ) showing binding of **11** and **9** to Cps2L. Asterisk indicates spectrum showing binding (peaks above baseline). Sample compositions (see General Methods). (A)  $^1\text{H}$  NMR spectrum of **11** and benzoic acid (control nonbinder). (B) **11** with Cps2L. (C)  $^1\text{H}$  NMR spectrum of **9** and benzoic acid. (D) **9** with Cps2L.

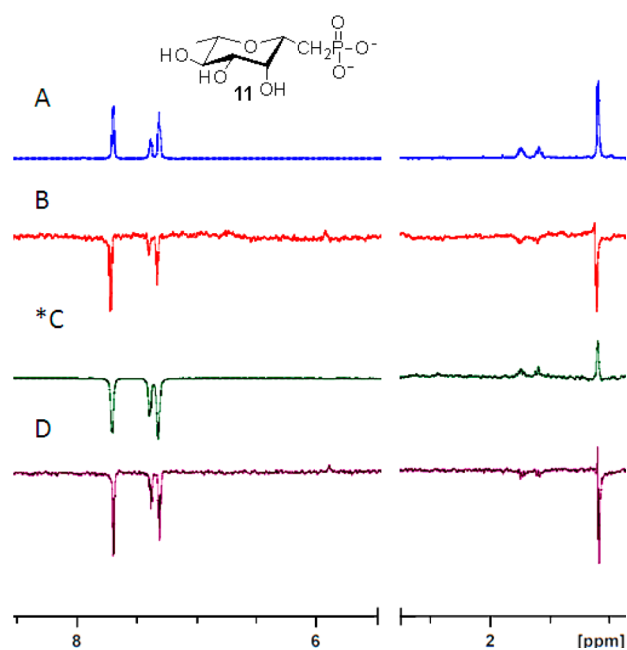


**Figure 7.** WaterLOGSY NMR spectra (700 MHz, 10:90  $\text{D}_2\text{O}/\text{H}_2\text{O}$ ) for **11**. Asterisk indicates spectrum showing binding. Sample compositions (see General Methods). (A)  $^1\text{H}$  NMR spectrum of **11** and benzoic acid. (B) **11** with RmlB. (C) **11** with RmlC. (D) **11** with RmlD.

necessary to facilitate the binding of **1** (Figure 8). However, analogue **11** was found to bind in the presence of substrate **1**, yet not in the presence of substrate **2**. This suggests that **11** may, in fact, be binding to the same site as substrate **1**, and that the conformational change induced by **2** might hinder the ability of **11** to bind Cps2L.

The WaterLOGSY spectra indicate binding of dTDP-Glc (**3**) to Cps2L (Figure 9A). In the time it took to prepare the

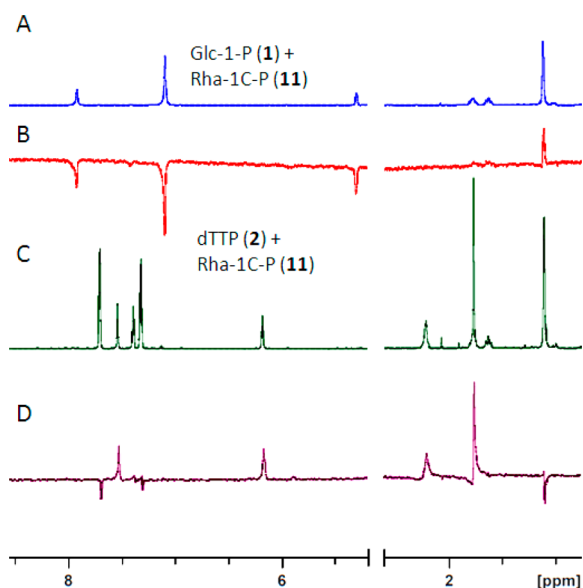


**Figure 8.** WaterLOGSY NMR spectra (700 MHz, 10:90 D<sub>2</sub>O/H<sub>2</sub>O) of **11** and substrate **1** or **2** with Cps2L. Sample compositions (see General Methods). (A) <sup>1</sup>H NMR spectra of **1** and **11**. (B) **11** binding to Cps2L, **1** nonbinding. (C) <sup>1</sup>H NMR spectrum of **2**, **11**, and benzoic acid with Cps2L. (D) **2** binding to Cps2L, **11** nonbinding.

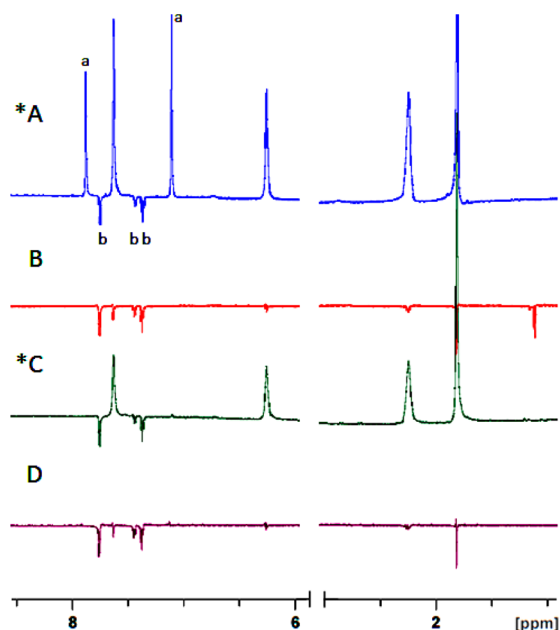


**Figure 9.** WaterLOGSY NMR spectra (700 MHz, 10:90 D<sub>2</sub>O/H<sub>2</sub>O) showing dTDP-Glc **3** binding or nonbinding. Sample compositions (see General Methods). Asterisk indicates spectra showing binding. (A) **3** with Cps2L. (B) **3** with RmlB. (C) **3** with RmlC. (D) **3** with RmlD. (a) Residual imidazole binding the His<sub>6</sub>-Tag on Cps2L. (b) Benzoic acid control nonbinder.

sample, RmlB turned **3** over to **4**, despite no additional NAD<sup>+</sup>, as demonstrated by the new peak at ~1 ppm for the methyl substituent (Figure 9B), and loss of the C4'' and C6'' proton signals (independently observed). These results are indicative that both the RmlB catalyzed oxidation and dehydration occurred, suggesting the enzyme contains endogenous NAD<sup>+</sup>. Binding of **3** to RmlC was clearly observed (Figure 9C), whereas, on the basis of the cancellation of signals, a weak binding to

RmlD was observed (Figure 9D). The WaterLOGSY spectra of dTDP-Rha (**6**) with Cps2L and RmlB-D is shown in Figure 10.

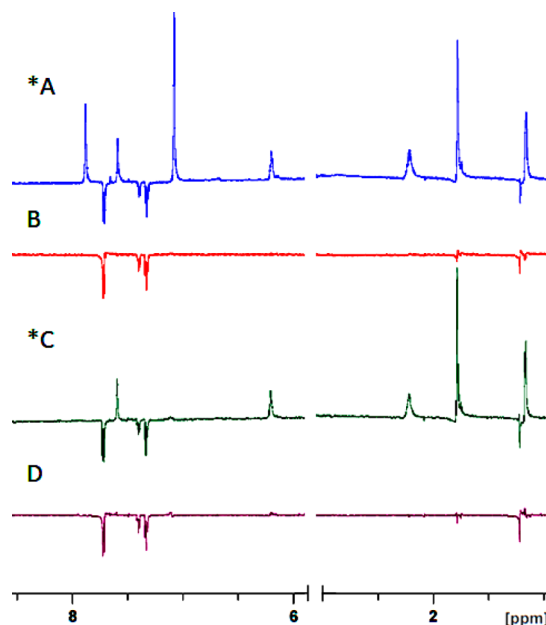


**Figure 10.** WaterLOGSY NMR spectra (700 MHz, 10:90 D<sub>2</sub>O/H<sub>2</sub>O) showing dTDP-Rha **6** binding (above baseline) or nonbinding (below baseline). Sample compositions (see General Methods). Asterisk indicates spectra showing binding. (A) **6** with Cps2L. (B) **6** with RmlB. (C) **6** with RmlC. (D) **6** with RmlD.

The product of RmlD is dTDP-Rha (**6**). dTDP-Rha (**6**) bound Cps2L as anticipated by crystallography and kinetic studies for homologous enzymes.<sup>14</sup> Unequivocal binding was also observed for **6** to RmlC. For RmlB and RmlD, we observed significant reduction in intensity of the signals for **6** relative to the benzoic acid control, and the signals for **6** were also difficult to phase and remained dispersive. As indicated above, this is likely due to weak binding of the enzymes.

**Enzyme Inhibition Studies.** Compounds **9** and **11** were first evaluated as Glc-1-P (**1**) analogue substrates for Cps2L given that the enzyme had previously demonstrated a broad substrate specificity,<sup>34,37,38</sup> including poor conversion (3–10%) observed for β-L-fucosyl phosphate.<sup>34</sup> Negligible turnover (<1%) to sugar nucleotide products were observed by HPLC over 24 h using 2–10 EU of Cps2L with a 8:1 ratio of **9** or **11** relative to dTTP substrate (**2**) (Supporting Information). This suggested that the L-rhamnose phosphonates did not act as substrates for Cps2L. Compounds **9**, **11**, **13**, **15**, and **18** were each evaluated as inhibitors of Cps2L at various concentrations between 0 and 100 mM against 10 mM concentrations of substrates **1** and **2**. The percentage conversion was calculated as the concentration of product formed (**3**) relative to the remaining starting material (**2**) for each concentration of inhibitor tested relative to a control reaction in which no inhibitor was present. IC<sub>50</sub> curves were generated for compounds **9**, **11**, and **13** (Supporting Information). Although compounds **15** and **18** did exhibit minor inhibition (<10%) at concentrations approaching 100 mM, IC<sub>50</sub> curves could not be generated within the concentration range sampled (0–100 mM). The IC<sub>50</sub> and K<sub>i</sub> values (as calculated using the Cheng–Prusoff equation<sup>39</sup>) are presented in Table 1.

It was found the L-rhamnose 1C-phosphonate analogue **11** exhibited the most potent inhibition (IC<sub>50</sub> = 5.7 mM) relative

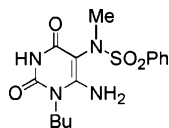
**Table 1.** Inhibition of Cps2L by L-Rhamnose Phosphonates

compound	IC <sub>50</sub> (mM)	K <sub>i</sub> <sup>a</sup> (μM) <sup>c</sup>	K <sub>i</sub> <sup>b</sup> (μM) <sup>c</sup>	pK <sub>a</sub> 2 <sup>d</sup>
9	23.9	295	358	6.5
11	5.7	70	85	7.0
13	18.3	225	274	5.7
15	>100 <sup>e</sup>			5.0
18	>100 <sup>e</sup>			5.0
24	>25 <sup>e</sup>			

<sup>a</sup>With respect to Glc-1-P. <sup>b</sup>With respect to dTTP. <sup>c</sup>Calculated using the Cheng–Prusoff equation<sup>39</sup> assuming competitive inhibition. <sup>d</sup>Estimated from previous pK<sub>a</sub>2 studies of analogous fluoro and nonfluoro gluco-phosphonate and ketosephosphonate analogues.<sup>27</sup> <sup>e</sup>IC<sub>50</sub> value beyond limit of inhibitor concentrations tested.

to ketosephosphonate **9** (IC<sub>50</sub> = 23.9 mM) and monofluoro ketosephosphonate **13** (IC<sub>50</sub> = 18.3 mM). This is likely due to the lack of the C2 axial hydroxyl moiety in the phosphonate scaffold, which may reduce inhibitor-enzyme binding efficiency for the ketosephosphonates. The presence and quantity of fluorine atoms (0–2) seems to have a significant impact on the potency of inhibition. The incorporation of fluorine into phosphonate analogues of natural phosphates has been shown to reduce the pK<sub>a</sub>2 of phosphonates by ~0.5–1 units per fluorine atom.<sup>27</sup> The assays were conducted at pH 7.5 to ensure complete ionization of phosphonate functionality. Monofluoro analogue **13** produced noticeably improved inhibition relative to its nonfluorinated analogue **9**. On the basis of previous studies of fluorinated ketosephosphonates,<sup>27</sup> the pK<sub>a</sub>2 values for these compounds were estimated to be ~5.7 and ~6.5 for **13** and **9**, respectively. The ability of ketosephosphonate **9** to undergo mutarotation, as determined by <sup>31</sup>P and <sup>1</sup>H NMR spectroscopy, relative to the exclusively α-pyranose analogue **13**, is also a probable factor in explaining the reduced inhibition observed for **9**. The fact that difluoro analogues **15** and **18** (pK<sub>a</sub>2 ~5.0) showed only minor inhibitory activity (<10%) relative to the other analogues (**9**, **11**, and **13**) suggests that the presence of an extra fluorine atom and additional pK<sub>a</sub>2 reduction is detrimental to inhibition.

Thymidyltransferases show high sequence homology (>60%) across various bacterial species (see sequence alignment, Supporting Information), with Cps2L (*S. pneumoniae*) and RmlA (*P. aeruginosa*) sharing 68% identity. Commercially available thymine analogue **24** (Figure 11) was shown to be a

**Figure 11.** Structure of RmlA (*P. aeruginosa*) inhibitor (**24**).

potent inhibitor of RmlA (*P. aeruginosa*). Naismith and co-workers report an IC<sub>50</sub> value of 0.32 μM for allosteric competitive inhibitor compound **24**.<sup>9</sup> We chose this compound as a benchmark for our synthesized compounds.

We determined, using the Cheng–Prusoff equation, a K<sub>i</sub> value of ~0.2 μM for both Glc-1-P and dTTP relative to RmlA for compound **24**. With RmlA and Cps2L being 68% identical, it was expected that comparable inhibition might be observed for Cps2L. Using the predicted K<sub>i</sub> for RmlA, an IC<sub>50</sub> value between 10–20 μM was predicted for our HPLC based Cps2L inhibition assay. A solution of **24** (50 mM in 1:1 DMSO/Tris–HCl,

pH 7.5) was prepared and used in the inhibition assays. Concentrations between 0 and 25 mM of **24** were tested in an attempt to determine an IC<sub>50</sub> value for **24** against Cps2L. All control samples were run in the absence of inhibitor **24** with equal volume proportions of DMSO to ensure any inhibition observed could not be attributed to solvent effects. For compound **24**, no inhibition was observed up to 20 mM. At 25 mM, minor inhibition (<10%) was observed. Due to the reduced solubility of **24** in Tris–HCl (pH 7.5) and reduced efficiency of Cps2L in the presence of increasing concentrations of DMSO (Supporting Information), concentrations beyond 25 mM of **24** were not investigated. Although compound **24** may be a poor inhibitor for Cps2L, its IC<sub>50</sub> is significantly higher than that of phosphonate and ketosephosphonate analogues **9**, **11**, and **13**. We were initially surprised that compound **24** failed to significantly inhibit Cps2L based on the high homology between Cps2L and RmlA. Compound **24** binds to the allosteric site in RmlA by interacting with seven key residues. These are Gly115, Phe118, His119, Lys249, Ala251, Cys252, and Glu255.<sup>9</sup> In Cps2L, only three of these residues are conserved (Gly115, Ala251, and Glu255), which could result in reduced binding and, consequently, poorer inhibition of Cps2L relative to RmlA in the presence of compound **24**.

The most potent phosphonate inhibitor (**11**) was subjected to a coupled spectrophotometric inhibition assay to determine the mode of inhibition with respect to substrates **1** and **2**. The Cps2L reaction was coupled with inorganic pyrophosphatase (IPP) to produce phosphate, which was used as a substrate for human purine nucleoside phosphorylase (PNP) along with 7-methyl-6-thioguanosine (MESG) (**25**) (λ<sub>max</sub> = 330 nm) to produce 7-methyl-6-thioguanine (**26**) (λ<sub>max</sub> = 355 nm) and α-D-ribose 1-phosphate (**27**). A coupled assay was necessary because Cps2L substrate **2** and product **3** have the same λ<sub>max</sub> value (254 nm). The coupled assay is shown in Scheme 3.<sup>40</sup> The kinetic parameters for Cps2L are displayed in Table 2. The K<sub>m</sub> value for **1** matched closely with previously reported studies using HPLC based assays.<sup>37</sup> The K<sub>m</sub> value for **2** with Cps2L has not been reported previously. Inhibitor **11** was found to be competitive with respect to **1** (K<sub>i</sub> = 536 μM) and uncompetitive with respect to **2** (K<sub>i</sub> = 497 μM) using the coupled assay method. The Michaelis–Menten and Lineweaver–Burk plots can be found in the Supporting Information. Both values were significantly higher than predicted from the Cheng–Prusoff equation and IC<sub>50</sub> values determined by the HPLC method, using only Cps2L.

On the basis of the coupled inhibition assay results, it is expected that inhibitor **11** binds to the same site as **1** both prior to (competitive model) and after (uncompetitive model) the conformational change induced by the binding of **2**. Although binding in the presence of **2** was not observed by WaterLOGSY NMR spectroscopy, it could be rationalized by Cps2L having higher affinity for **2** (K<sub>m,app</sub> = 152 μM) relative to **11** (K<sub>i</sub> = 497 μM). Past<sup>15</sup> and recent<sup>9</sup> studies of nucleotidyltransferase inhibition have all focused on the study of allosteric inhibitor compounds with a common trend being that each of the allosteric binders contained a thymine derived moiety necessary for binding. The scaffold of inhibitor **11** is more similar to substrate **1**, with no thymine component. To our knowledge, it is the first reported sugar–phosphonate active site binding competitive inhibitor of Cps2L. The synthesis of the sugar nucleotide analogues of **9**, **11**, and **13** would produce analogues of dTDP-Rha (**6**). These analogues would be predicted to be more potent inhibitors than their phosphonate analogues and, with the introduction of the thymidine



Scheme 3. Cps2L, IPP, and Human PNP Coupled Assay

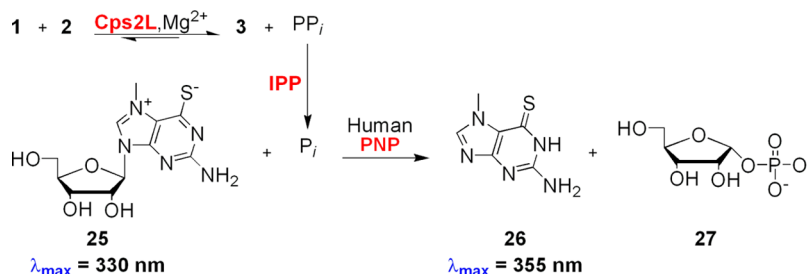


Table 2. Apparent Substrate Kinetics and Inhibition Parameters for Cps2L in the Presence of 11

compound	$K_{\text{m,app}}$ ( $\mu\text{M}$ )	$K_i$ ( $\mu\text{M}$ )	$k_{\text{cat}}$ ( $\text{s}^{-1}$ )	$k_{\text{cat}}/K_{\text{m}}$ ( $\text{s}^{-1} \mu\text{M}^{-1}$ )
1	125 <sup>a,c</sup> 139 <sup>a,d</sup>		60 <sup>c</sup>	0.475 <sup>c</sup>
2	152 <sup>b,c</sup>		54 <sup>c</sup>	0.352 <sup>c</sup>
11		536 <sup>a,e</sup> 497 <sup>b,f</sup>		

<sup>a</sup>With respect to variable Glc-1-P. <sup>b</sup>With respect to variable dTTP.

<sup>c</sup>Calculated from coupled spectrophotometric assay. <sup>d</sup>Previously reported.<sup>37</sup> <sup>e</sup>Competitive inhibition. <sup>f</sup>Uncompetitive inhibition.

component into their scaffolds, would potentially function as allosteric competitive inhibitors.

## CONCLUSION

We have reported the synthesis and enzymatic evaluation of a series of L-rhamnose 1C-phosphonate and ketosephosphonate analogues and investigated the impact of fluorination on the inhibition of nucleotidyltransferase Cps2L. WaterLOGSY studies with compounds **9** and **11** demonstrated the potential of synthetic substrate analogues to bind to multiple enzymes within a single biosynthetic pathway. WaterLOGSY studies of dTDP-Glc (**3**) and dTDP-Rha (**6**) also highlighted the capacity for sugar nucleotides to bind to, and potentially inhibit, multiple enzymes within a single bacterial biosynthetic pathway. The synthesized compounds bound multiple enzymes in the L-rhamnose pathway and were competitive inhibitors for the first enzyme, Cps2L. L-Rhamnose-1C-phosphonate (**11**) was found to be a better inhibitor than all of the ketosephosphonates, presumably due to reduced binding efficiency from the presence of the C2 hydroxyl group on the ketosephosphonate scaffold. For the series of ketosephosphonates, the presence of one fluorine atom at the C1 position improved inhibition by ~25% relative to the nonfluorinated phosphonate whereas the presence of two fluorine atoms was detrimental to inhibition. We expect the sugar nucleotide analogues of these L-rhamnose phosphonate and ketosephosphonate analogues will significantly magnify their capacity to inhibit Cps2L and potentially other enzymes within the prokaryote L-rhamnose biosynthetic pathway. Such studies are currently in progress and results will be reported in due course.

## EXPERIMENTAL SECTION

**General Methods.** All reagents and solvents were purchased and used without further purification. Synthetic reactions were performed under N<sub>2</sub> atmosphere unless otherwise indicated. Dibenzyl methylphosphonate was prepared and characterized as previously described.<sup>31</sup> Reaction progress was generally monitored by thin layer chromatography. Plates were visualized using an ethanol dipping solution containing *p*-anisaldehyde (3.4%), sulfuric acid (2.2%), and acetic acid

(1.1%) followed by charring. Either 300 or 500 MHz NMR spectrometers were used for all structural NMR data. Peak assignments were aided by <sup>1</sup>H–<sup>1</sup>H correlated spectroscopy (COSY) and <sup>1</sup>H–<sup>13</sup>C heteronuclear single quantum coherence (HSQC) experiments when necessary. 1D NOESY was used to determine stereochemistry for select compounds. A 700 MHz spectrometer equipped with a 1.7 mm CryoProbe was utilized for all WaterLOGSY binding experiments. HPLC analysis for all enzymatic inhibition assays was performed as previously described.<sup>34</sup> Compounds containing a nucleotide base chromophore were monitored at 254 nm absorbance. HPLC runs were performed for 15 min at a flow rate of 1 mL/min. A linear gradient from 90:10 A/B to 40:60 A/B over 8 min followed by a 40:60 A/B plateau from 8 to 10 min and a linear decline to 90:10 A/B from 10 to 11 min followed by isocratic 90:10 A/B was used for all assays. Buffer A was aqueous 12 mM Bu<sub>4</sub>NBr, 10 mM KH<sub>2</sub>PO<sub>4</sub>, and 5% HPLC grade CH<sub>3</sub>CN. Buffer B was HPLC grade CH<sub>3</sub>CN. Low resolution mass spectra were obtained with a hybrid triple quadrupole linear ion trap ionization (ESI) source. Samples were run using a flow rate of 120  $\mu\text{L}/\text{min}$  and an isocratic 70:30 CH<sub>3</sub>CN/2 mM aqueous ammonium acetate (pH 5.5) buffer. The capillary voltage was set to  $\pm 4500$  kV, with a declustering potential of  $\pm 60$  V and a curtain gas of 20 (arbitrary units) for positive and negative mode, respectively. Analyst version 1.4.1 (Applied Biosystem) software was used for analysis.

**WaterLOGSY NMR Analysis.** WaterLOGSY NMR samples were composed of binding substrates Glc-1-P (5 mM) and/or dTTP (5 mM) with MgCl<sub>2</sub> (5 mM) co-factor or sugar nucleotides (5 mM) with MgCl<sub>2</sub> (5 mM) and enzymes Cps2L, RmlB, RmlC, or RmlD (0.05 mM). Benzoic acid (5 mM) was used as a control nonbinder for all experiments. For experiments using phosphonate inhibitors, 5 mM concentrations were used. All samples were prepared in Tris–HCl (100 mM, pH 7.4) buffer with 10% D<sub>2</sub>O to a total volume of 50  $\mu\text{L}$ . Benzoic acid was used as a control nonbinder with the exception of the competitive model of Glc-1-P (**1**) and Rha-1C-P (**11**) (Figure 8). In each spectrum, proton signals for the Tris–HCl buffer (~3.5 ppm) appear as the major signal in the <sup>1</sup>H NMR spectra. In spectra containing Cps2L, residual signals of imidazole left over from purification (~7.1 and 7.8 ppm) could not be removed and should not be confused with thymidine or benzoic acid aromatic proton signals.

**HPLC Enzyme Assay and Inhibition Conditions.** Cps2L, RmlB–D were overexpressed and purified as previously described.<sup>34,41</sup> The concentration of Cps2L was measured spectrophotometrically at 280 nm using a calculated extinction coefficient of 29.8 mM<sup>-1</sup> cm<sup>-1</sup>. All stock solutions were prepared in Tris–HCl buffer (100 mM, pH 7.4). Inhibition assays were conducted using phosphonate analogues (0–100 mM), or compound **24** (0–25 mM) with Glc-1-P (10 mM), dTTP (10 mM), MgCl<sub>2</sub> (20 mM), and Cps2L (8 EU) in a final volume of 50  $\mu\text{L}$  of Tris–HCl buffer. Samples were incubated for 17 min at 37 °C, at which point 25  $\mu\text{L}$  aliquots were quenched in an equal volume of HPLC grade MeOH. Conversions were approximately 30% after 17 min. In the case of compound **24**, a concentrated stock solution (50 mM in 1:1 DMSO/Tris–HCl, pH 7.5) was used. IC<sub>50</sub> curves and values were generated based on HPLC conversion using Graft 5 Eritacus software.  $K_i$  values were approximated relative to Glc-1-P and dTTP substrates using the Cheng–Prusoff equation, which assumes a competitive mode of inhibition. Due to the time intensive requirements of performing HPLC-based inhibition assays, we did not carry out experiments in duplicate.



**Spectrophotometric Enzyme Coupled Kinetic and Inhibition**

**Assay Conditions.** Recombinant human PNP was overexpressed and purified using the same procedure as described for Cps2L and RmlB-D, with the following modifications; overnight induction at 37 °C was initiated with 0.1% w/v lactose.<sup>42</sup> The concentration of PNP was measured spectrophotometrically at 280 nm using an extinction coefficient of 29.8 mM<sup>-1</sup> cm<sup>-1</sup>. Inorganic pyrophosphatase (IPP) from *Escherichia coli* was purchased from a supplier. Stock solutions of 0.1 EU/μL IPP were prepared in Millipore water and stored at -30 °C. Thawed aliquots were kept in a fridge and were used for up to 1 month after thawing. MESH was purchased from a supplier. MESH stock solutions were prepared in Millipore water no more than 2 weeks prior to use and aliquots were stored at -30 °C. MESH solutions were used as soon as possible after thawing. All other stock solutions were prepared in Tris-HCl buffer (50 mM, pH 7.5). Enzyme kinetic assays were performed for each substrate, dTTP and Glc-1-P. Reactions containing 1 mM Glc-1-P or dTTP, 0–300 μM dTTP or Glc-1-P, 8 μM Human PNP, 0.05 EU IPP, 5.6 mM MgCl<sub>2</sub>, and 400 μM MESH in 50 mM Tris-HCl (pH 7.5) were initiated by the addition of 4.9 nM Cps2L. Assays were made to a final reaction volume of 80 μL and performed in a 384 well plate. Initial velocities were monitored continuously by UV spectrometry at λ = 360 nm using Softmax pro 4.8. Inhibition assays were performed using the same reaction conditions with variable concentrations (250–1000 μM) of Rha-1C-P. Initial velocities were converted from mAU/min to μM/min using a 0–100 μM P<sub>i</sub> standard curve. Michaelis-Menten and inhibition equations were fit using Graft 5 Erithacus Software.

**Synthetic Procedures and Characterizations.** *Dimethyl (3,4,5-Tri-O-benzyl-1-deoxy-α-L-rhamno-heptulopyranosyl)phosphonate (8a)*. Dimethyl methylphosphonate (0.93 mL, 8.31 mmol) was dissolved in anhydrous THF (5 mL) under nitrogen, and the mixture was cooled to -78 °C using a dry ice/acetone slurry. *n*-Butyllithium (2.5 M in hexane) (0.35 mL, 8.31 mmol) was added, and the solution was stirred for 30 min before 2,3,4-tri-O-benzyl-L-rhamno-1,5-lactone (7) (1.197 g, 2.8 mmol) was added dropwise in a solution of THF (5 mL). After 75 min, TLC showed complete consumption of 7. The reaction was quenched with 10% NH<sub>4</sub>Cl (10 mL), and the THF layer was extracted from the mixture. The aqueous layer was then extracted from the mixture with CH<sub>2</sub>Cl<sub>2</sub> (3 × 10 mL). The organic extracts were combined, dried (Na<sub>2</sub>SO<sub>4</sub>), and concentrated. The result material was purified using column chromatography (40:60 EtOAc/hexane) to afford the product (8a) as a clear liquid (1.378 g, 88% yield): *R*<sub>f</sub> = 0.25 (40:60 EtOAc/hexane); δ<sub>H</sub> (CDCl<sub>3</sub>) 7.20–7.50 (m, 15H, 3 × C<sub>6</sub>H<sub>5</sub>), 5.74 (s, 1H, OH), 4.50–5.10 (m, 6H, 3 × CH<sub>2</sub>Ph), 4.12 (dd, 1H, H4, <sup>3</sup>J<sub>4,5</sub> = 9.4 Hz, <sup>3</sup>J<sub>4,3</sub> = 2.7 Hz), 4.03 (m, 1H, H6), 3.83 (d, 3H, OCH<sub>3</sub>, <sup>3</sup>J<sub>H,P</sub> = 11.1 Hz), 3.76 (d, 1H, H3, <sup>3</sup>J<sub>3,4</sub> = 2.7 Hz), 3.69 (d, 3H, OCH<sub>3</sub>, <sup>3</sup>J<sub>H,P</sub> = 11.1 Hz), 3.64 (t, 1H, H5, <sup>3</sup>J<sub>5,4</sub> = <sup>3</sup>J<sub>5,6</sub> = 9.4 Hz), 2.60 (dd, 1H, H1a, <sup>2</sup>J<sub>H,P</sub> = 17.9 Hz, <sup>2</sup>J<sub>H,H</sub> = 16.0 Hz), 1.69 (dd, 1H, H1b, <sup>2</sup>J<sub>H,P</sub> = 17.9 Hz, <sup>2</sup>J<sub>H,H</sub> = 16.0 Hz) 1.32 (d, 3H, H7, <sup>3</sup>J<sub>7,6</sub> = 6.4 Hz); δ<sub>C</sub> 138.3–138.8 (3 × C, C<sub>6</sub>H<sub>5</sub>), 127.5–129.0 (15 × CH, C<sub>6</sub>H<sub>5</sub>), 97.1 (d, C, C2, <sup>2</sup>J<sub>C,P</sub> = 7.6 Hz), 81.5 (CH, C4), 80.3 (CH, C5), 78.2 (d, CH, C3, <sup>3</sup>J<sub>C,P</sub> = 12.5 Hz), 75.4 (CH<sub>2</sub>, CH<sub>2</sub>Ph), 74.8 (CH<sub>2</sub>, CH<sub>2</sub>Ph), 73.2 (CH<sub>2</sub>, CH<sub>2</sub>Ph), 69.0 (CH, C6), 53.9 (d, CH<sub>3</sub>, OCH<sub>3</sub>, <sup>2</sup>J<sub>C,P</sub> = 5.8 Hz), 51.8 (d, CH<sub>3</sub>, OCH<sub>3</sub>, <sup>2</sup>J<sub>C,P</sub> = 5.8 Hz), 33.2 (d, CH<sub>2</sub>, C1, <sup>1</sup>J<sub>C,P</sub> = 135.12 Hz), 18.0 (CH<sub>3</sub>, C7); δ<sub>p</sub> 32.22 (s, 1P). HRMS (ESI<sup>-</sup>): found [M - H]<sup>-</sup> 555.2164. C<sub>30</sub>H<sub>36</sub>O<sub>8</sub>P<sub>1</sub> requires [M - H]<sup>-</sup> 555.2153.

*Dibenzyl (3,4,5-Tri-O-benzyl-1-deoxy-α-L-rhamno-heptulopyranosyl)phosphonate (8b)*. Dibenzyl methylphosphonate (0.374 g, 1.35 mmol) was dissolved in anhydrous THF (5 mL) under nitrogen, and the mixture was cooled to -78 °C using a dry ice/acetone slurry. *n*-Butyllithium (0.5 mL, 1.25 mmol) was added, and the solution was stirred for 30 min before 2,3,4-tri-O-benzyl-L-rhamno-1,5-lactone (7) (0.220 g, 0.5 mmol) was added dropwise in a solution of THF (1 mL). After 75 min, TLC showed complete consumption of (7). The reaction was quenched with 10% NH<sub>4</sub>Cl (10 mL), and the THF layer was extracted from the mixture. The aqueous layer was then extracted from the mixture with CH<sub>2</sub>Cl<sub>2</sub> (3 × 10 mL). The organic extracts were combined, dried (Na<sub>2</sub>SO<sub>4</sub>), and concentrated. The resulting material was purified using column chromatography (25:75 EtOAc/hexane) to afford the product as a clear viscous liquid (8b) (0.270 g, 76% yield):

*R*<sub>f</sub> = 0.22 (20:80 EtOAc/hexane); δ<sub>H</sub> 7.25–7.45 (m, 25H, 5 × C<sub>6</sub>H<sub>5</sub>), 5.80 (s, 1H, OH), 4.60–5.24 (m, 10H, 5 × CH<sub>2</sub>Ph), 4.23 (dd, 1H, H4, <sup>3</sup>J<sub>4,5</sub> = 9.3 Hz, <sup>3</sup>J<sub>4,3</sub> = 2.6 Hz), 4.10 (m, 1H, H6), 3.76 (d, 1H, H3, <sup>3</sup>J<sub>3,4</sub> = 2.6 Hz), 3.67 (t, 1H, H5, <sup>3</sup>J<sub>5,4</sub> = <sup>3</sup>J<sub>5,6</sub> = 9.5 Hz), 2.70 (dd, 1H, H1a, <sup>2</sup>J<sub>H,P</sub> = 18.8 Hz, <sup>2</sup>J<sub>H,H</sub> = 15.4 Hz), 1.78 (dd, 1H, H1b, <sup>2</sup>J<sub>H,P</sub> = 18.8 Hz, <sup>2</sup>J<sub>H,H</sub> = 15.7 Hz), 1.37 (d, 3H, H7, <sup>3</sup>J<sub>7,6</sub> = 6.3 Hz); δ<sub>C</sub> 135.8–138.8 (5 × C, C<sub>6</sub>H<sub>5</sub>), 127.5–129.2 (25 × CH, C<sub>6</sub>H<sub>5</sub>), 97.3 (d, C, C2, <sup>2</sup>J<sub>C,P</sub> = 7.72 Hz), 81.4 (CH, C4), 80.4 (CH, C5), 78.5 (d, CH, C3, <sup>3</sup>J<sub>C,P</sub> = 12.77 Hz), 75.4 (CH<sub>2</sub>, CH<sub>2</sub>Ph), 74.9 (CH<sub>2</sub>, CH<sub>2</sub>Ph), 73.1 (CH<sub>2</sub>, CH<sub>2</sub>Ph), 69.0 (CH, C6), 68.5 (d, CH<sub>2</sub>, POCH<sub>2</sub>Ph, <sup>2</sup>J<sub>C,P</sub> = 5.5 Hz), 66.9 (d, CH<sub>2</sub>, POCH<sub>2</sub>Ph, <sup>2</sup>J<sub>C,P</sub> = 5.5 Hz), 34.3 (d, CH<sub>2</sub>, C1, <sup>1</sup>J<sub>C,P</sub> = 136.40 Hz), 18.0 (CH<sub>3</sub>, C7); δ<sub>p</sub> 30.49 (s, 1P). HRMS (ESI<sup>-</sup>): found [M - H]<sup>-</sup> 707.2762. C<sub>42</sub>H<sub>44</sub>O<sub>8</sub>P<sub>1</sub> requires [M - H]<sup>-</sup> 707.2779.

*Dimethyl (2,6-Anhydro-3,4,5-tri-O-benzyl-1-deoxy-L-rhamno-hept-1-enopyranosyl)phosphonate (10a)*. Dimethyl (tri-O-benzyl-1-deoxy-L-rhamno-heptulopyranosyl)phosphonate (8a) (0.660 g, 1.18 mmol) was dissolved in a mixture of 7:2 CH<sub>2</sub>Cl<sub>2</sub>:pyridine (9 mL), and methyl oxalyl chloride (MeOXCl) (1.13 mL, 10.58 mmol) was added to the mixture dropwise with stirring under nitrogen. After 90 min, TLC showed complete consumption of 8a so the reaction was quenched with EtOH (1 mL) and was allowed to stir for 10 min before CH<sub>2</sub>Cl<sub>2</sub> (13 mL) and NaHCO<sub>3</sub> (5 mL, sat.) were added. The reaction was stirred for an additional 5 min after which the mixture was poured into NaHCO<sub>3</sub> (10 mL) and extracted with CH<sub>2</sub>Cl<sub>2</sub> (3 × 15 mL) before being dried (Na<sub>2</sub>SO<sub>4</sub>) and concentrated. The resulting material was purified using column chromatography (70:30–100:0 EtOAc/hexane) to afford the product (10a) as a clear viscous liquid (0.433 g, 68% yield): *R*<sub>f</sub> = 0.46 (80:20 EtOAc/hexane); δ<sub>H</sub> (CD<sub>2</sub>Cl<sub>2</sub>) 7.20–7.50 (m, 15H, 3 × C<sub>6</sub>H<sub>5</sub>), 5.02 (d, 1H, H1, <sup>2</sup>J<sub>H,P</sub> = 12.4 Hz), 4.40–4.80 (m, 6H, 3 × CH<sub>2</sub>Ph), 4.19 (d, 1H, H3, <sup>3</sup>J<sub>3,4</sub> = 2.8 Hz), 3.89 (m, 1H, H6), 3.80 (dd, 1H, H4, <sup>3</sup>J<sub>4,5</sub> = 5.6 Hz, <sup>3</sup>J<sub>4,3</sub> = 2.8 Hz), 3.75 (dd, 6H, 2 × OCH<sub>3</sub>, <sup>3</sup>J<sub>H,P</sub> = 11.4 Hz, <sup>5</sup>J<sub>H,H</sub> = 1.1 Hz), 3.70 (dd, 1H, H5, <sup>3</sup>J<sub>5,6</sub> = 8.7 Hz, <sup>3</sup>J<sub>5,4</sub> = 5.6 Hz), 1.46 (d, 3H, H7, <sup>3</sup>J<sub>7,6</sub> = 6.2 Hz); δ<sub>C</sub> 165.75 (C, C2), 137.3–138.0 (3 × C, C<sub>6</sub>H<sub>5</sub>), 127.5–129.0 (15 × CH, C<sub>6</sub>H<sub>5</sub>), 92.8 (d, CH, C1, <sup>1</sup>J<sub>C,P</sub> = 191.4 Hz), 80.5 (CH, C5), 78.1 (CH, C4), 75.9 (CH, C6), 75.2 (d, CH, C3, <sup>3</sup>J<sub>C,P</sub> = 14.9 Hz), 73.8 (CH<sub>2</sub>, CH<sub>2</sub>Ph), 72.4 (CH<sub>2</sub>, CH<sub>2</sub>Ph), 71.5 (CH<sub>2</sub>, CH<sub>2</sub>Ph), 52.7 (d, CH<sub>3</sub>, OCH<sub>3</sub>, <sup>2</sup>J<sub>C,P</sub> = 5.5 Hz), 52.3 (d, CH<sub>3</sub>, OCH<sub>3</sub>, <sup>2</sup>J<sub>C,P</sub> = 5.5 Hz), 19.1 (CH<sub>3</sub>, C7); δ<sub>p</sub> 20.17 (s, 1P). HRMS (ESI<sup>+</sup>): found [M + Na]<sup>+</sup> 561.2009. C<sub>30</sub>H<sub>35</sub>O<sub>7</sub>P<sub>1</sub> requires [M + Na]<sup>+</sup> 561.2013.

*Dibenzyl (2,6-Anhydro-3,4,5-tri-O-benzyl-1-deoxy-L-rhamno-hept-1-enopyranosyl)phosphonate (10b)*. Dibenzyl (tri-O-benzyl-1-deoxy-L-rhamno-heptulopyranosyl)phosphonate (8b) (0.318 g, 0.45 mmol) was dissolved in a mixture of 7:2 CH<sub>2</sub>Cl<sub>2</sub>:pyridine (7 mL), and methyl oxalyl chloride (MeOXCl) (0.4 mL, 4.18 mmol) was added to the mixture dropwise with stirring under nitrogen. After 90 min, TLC analysis showed complete consumption of the starting material so the reaction was quenched with EtOH (0.5 mL) and was allowed to stir for 10 min before CH<sub>2</sub>Cl<sub>2</sub> (13 mL) and NaHCO<sub>3</sub> (5 mL, sat.) were added. The reaction mixture was stirred for an additional 5 min after which it was poured into NaHCO<sub>3</sub> (10 mL, sat.) and extracted with CH<sub>2</sub>Cl<sub>2</sub> (3 × 15 mL) before being dried (Na<sub>2</sub>SO<sub>4</sub>) and concentrated. The result material was purified using column chromatography (35:65 EtOAc/hexane) to afford the product as a clear viscous liquid (10b) (0.188 g, 60% yield): *R*<sub>f</sub> = 0.44 (50:50 EtOAc/hexane); δ<sub>H</sub> (CD<sub>2</sub>Cl<sub>2</sub>) 7.00–7.20 (m, 25H, 5 × C<sub>6</sub>H<sub>5</sub>), 4.86 (d, 1H, H1, <sup>2</sup>J<sub>H,P</sub> = 12.7 Hz), 4.20–4.80 (m, 10H, 5 × CH<sub>2</sub>Ph), 4.01 (d, 1H, H3, <sup>3</sup>J<sub>3,4</sub> = 1.8 Hz), 3.58 (m, 2H, H4, H6), 3.37 (dd, 1H, H5, <sup>3</sup>J<sub>5,6</sub> = 8.5 Hz, <sup>3</sup>J<sub>5,4</sub> = 4.6 Hz), 1.11 (d, 3H, H7, <sup>3</sup>J<sub>7,6</sub> = 6.4 Hz); δ<sub>C</sub> 165.6 (C, C2), 137.5–138.7 (5 × C, C<sub>6</sub>H<sub>5</sub>), 128.0–129.2 (25 × CH, C<sub>6</sub>H<sub>5</sub>), 92.2 (d, CH, C1, <sup>1</sup>J<sub>C,P</sub> = 190.9 Hz), 81.2 (CH, C5), 78.2 (CH, C4), 78.0 (d, CH, C3, <sup>3</sup>J<sub>C,P</sub> = 14.5 Hz), 75.8 (CH, C6), 73.7 (CH<sub>2</sub>, CH<sub>2</sub>Ph), 72.8 (CH<sub>2</sub>, CH<sub>2</sub>Ph), 72.3 (CH<sub>2</sub>, CH<sub>2</sub>Ph), 67.6 (d, CH<sub>2</sub>, POCH<sub>2</sub>Ph, <sup>2</sup>J<sub>C,P</sub> = 5.0 Hz), 67.3 (d, CH<sub>2</sub>, POCH<sub>2</sub>Ph, <sup>2</sup>J<sub>C,P</sub> = 5.0 Hz), 19.2 (CH<sub>3</sub>, C7); δ<sub>p</sub> 17.78 (s, 1P). HRMS (ESI<sup>+</sup>): found [M + Na]<sup>+</sup> 713.2606. C<sub>42</sub>H<sub>43</sub>O<sub>7</sub>P<sub>1</sub> requires [M + Na]<sup>+</sup> 713.2639.

*Dimethyl (3,4,5-Tri-O-benzyl-1-deoxy-1-R-fluoro-α-L-rhamno-heptulopyranosyl)phosphonate (12a)*. Dimethyl (2,6-anhydro-tri-O-benzyl-1-deoxy-L-rhamno-hept-1-enopyranosyl)phosphonate (10a) (0.250 g, 0.464 mmol) was dissolved in acetonitrile (5 mL), and

Selectfluor (0.350 g, 0.99 mmol) was added to the mixture all at once with stirring overnight at room temperature under nitrogen. Water (2 mL) was then added, and the solution was heated at 70 °C for 2.5 h before being poured into water (10 mL) and extracted with CH<sub>2</sub>Cl<sub>2</sub> (2 × 10 mL). The organic layer was dried (Na<sub>2</sub>SO<sub>4</sub>), concentrated, and purified using column chromatography (25:75 EtOAc/hexane) to afford the single stereoisomer (**12a**) (0.141 g, 54% yield):  $R_f = 0.24$  (30:70 EtOAc/hexane). By NOE analysis, the CHFP stereocenter was determined to be *R* configuration.  $\delta_{\text{H}}$ : (CDCl<sub>3</sub>) 7.20–7.50 (m, 15H, 3 × C<sub>6</sub>H<sub>5</sub>), 5.57 (s, 1H, OH), 4.50–5.10 (m, 7H, 3 × CH<sub>2</sub>Ph, H1), 4.15 (dd, 1H, H4  $^3J_{4,5} = 9.1$  Hz,  $^3J_{4,3} = 2.7$  Hz), 4.09 (m, 2H, H3, H6), 3.91 (d, 3H, OCH<sub>3</sub>,  $^3J_{\text{H,P}} = 11.1$  Hz), 3.84 (d, 3H, OCH<sub>3</sub>,  $^3J_{\text{H,P}} = 11.1$  Hz), 3.68 (t, 1H, H5,  $^3J_{5,4} = ^3J_{5,6} = 9.1$  Hz), 1.31 (d, 3H, H7,  $^3J_{7,6} = 6.2$  Hz).  $\delta_{\text{C}}$ : 138.4–138.8 (3 × C, C<sub>6</sub>H<sub>5</sub>), 127.5–129.0 (15 × CH, C<sub>6</sub>H<sub>5</sub>), 97.9 (d, C, C2,  $^2J_{\text{C,F}} = 24.7$  Hz), 85.8 (m, CH, C1), 81.2 (CH, C4), 80.1 (CH, C5), 75.4 (dd, CH, C3,  $^3J_{\text{C,F}} = 19.5$  Hz,  $^3J_{\text{C,P}} = 13.7$  Hz), 72.8 (CH<sub>2</sub>, CH<sub>2</sub>Ph), 69.4 (CH, C6), 54.4 (d, CH<sub>3</sub>, OCH<sub>3</sub>,  $^2J_{\text{C,P}} = 5.9$  Hz), 54.1 (d, CH<sub>3</sub>, OCH<sub>3</sub>,  $^2J_{\text{C,P}} = 5.9$  Hz), 17.9 (CH<sub>3</sub>, C7).  $\delta_{\text{P}}$ : 20.60 (d, 1P,  $^2J_{\text{P,F}} = 74.8$  Hz).  $\delta_{\text{F}}$ : -216.8 (d, 1F,  $^2J_{\text{F,P}} = 75.1$  Hz). HRMS (ESI<sup>-</sup>): found [M - H]<sup>-</sup> 573.2045. C<sub>30</sub>H<sub>35</sub>F<sub>2</sub>O<sub>8</sub>P<sub>1</sub> requires [M - 1]<sup>-</sup> 573.2059.

**Dibenzyl (3,4,5-Tri-*O*-benzyl-1-deoxy-1-*R*-fluoro- $\alpha$ -*L*-rhamno-heptulopyranosyl)phosphonate (12b).** Dibenzyl (2,6-anhydro-tri-*O*-benzyl-1-deoxy-*L*-rhamno-hept-1-enopyranosyl)phosphonate (**10b**) (0.142 g, 0.206 mmol) was dissolved with acetonitrile (3 mL), and Selectfluor (0.157 g, 0.44 mmol) was added to the mixture all at once with stirring overnight at room temperature under nitrogen. Water (1 mL) was then added, and the solution was heated at 70 °C for 2.5 h before being poured into water (10 mL) and extracted with CH<sub>2</sub>Cl<sub>2</sub> (2 × 10 mL). The organic layer was dried (Na<sub>2</sub>SO<sub>4</sub>), concentrated, and purified using column chromatography (16:84 EtOAc/hexane) to afford the *R* (**12b**) as a clear viscous liquid (0.033 g, 22% yield):  $R_f = 0.45$  (20:80 EtOAc/hexane);  $\delta_{\text{H}}$  (CDCl<sub>3</sub>) 7.29–7.45 (m, 25H, 5 × C<sub>6</sub>H<sub>5</sub>), 5.66 (s, 1H, OH), 4.63–5.25 (m, 11H, 5 × CH<sub>2</sub>Ph, H1), 4.17 (dd, 1H, H4  $^3J_{4,5} = 9.6$  Hz,  $^3J_{4,3} = 2.7$  Hz), 4.08–4.15 (m, 2H, H3, H6), 3.69 (t, 1H, H5,  $^3J_{5,4} = ^3J_{5,6} = 9.6$  Hz), 1.30 (d, 3H, H7,  $^3J_{7,6} = 6.3$  Hz);  $\delta_{\text{C}}$ : 135.0–139.0 (5 × C, C<sub>6</sub>H<sub>5</sub>), 127.6–129.1 (25 × CH, C<sub>6</sub>H<sub>5</sub>), 98.1 (d, C, C2,  $^2J_{\text{C,F}} = 25.2$  Hz), 85.1 (m, CH, C1), 81.3 (CH, C4), 80.2 (CH, C5), 75.4 (dd, CH, C3,  $^3J_{\text{C,F}} = 25.8$  Hz,  $^3J_{\text{C,P}} = 12.8$  Hz), 72.8 (CH<sub>2</sub>, CH<sub>2</sub>Ph), 69.4 (CH, C6), 69.2 (d, CH<sub>2</sub>, POCH<sub>2</sub>Ph,  $^2J_{\text{C,P}} = 6.4$  Hz), 69.0 (d, CH<sub>2</sub>, POCH<sub>2</sub>Ph,  $^2J_{\text{C,P}} = 6.4$  Hz), 18.0 (CH<sub>3</sub>, C7);  $\delta_{\text{P}}$ : 18.92 (d, 1P,  $^2J_{\text{P,F}} = 76.5$  Hz);  $\delta_{\text{F}}$ : -215.70 (d, 1F,  $^2J_{\text{F,P}} = 76.2$  Hz). HRMS (ESI<sup>-</sup>): found [M - 1]<sup>-</sup> 725.2668. C<sub>42</sub>H<sub>43</sub>F<sub>2</sub>O<sub>8</sub>P<sub>1</sub> requires [M - 1]<sup>-</sup> 725.2685.

**Diethyl (3,4,5-Tri-*O*-benzyl-1-deoxy-1,1-difluoro- $\alpha$ -*L*-rhamno-heptulopyranosyl)phosphonate (14).** Diisopropylamine (0.49 mL, 2.9 mmol) was dissolved in anhydrous THF (3 mL), and the mixture was cooled to -78 °C using a dry ice/acetone slurry. *n*-Butyllithium (1.2 mL, 2.9 mmol) was added, and the solution was stirred for 5 min before being transferred to an ice bath and allowed to warm to 0 °C over the course of 30 min. Diethyl difluoromethylphosphonate (0.5 mL, 3.2 mmol) was cooled to -78 °C in THF (2 mL) and added dropwise to the solution of LDA at -78 °C. After stirring for 15 min, 2,3,4-tri-*O*-benzyl-*L*-rhamno-1,5-lactone (**7**) (0.40 g, 0.93 mmol) in THF (3 mL) was added dropwise to the solution. TLC analysis showed complete consumption of the lactone after 30 min. The reaction was quenched with 10% NH<sub>4</sub>Cl (15 mL) followed by addition of diethyl ether. The aqueous layer was removed and extracted with diethyl ether (3 × 15 mL). The organic extracts were combined, dried (Na<sub>2</sub>SO<sub>4</sub>), and concentrated. The resulting material was purified using column chromatography (24:76 EtOAc/hexane) to afford the product as a clear viscous liquid (**14**) (0.423 g, 74% yield):  $R_f = 0.37$  (25:75 EtOAc/hexane);  $\delta_{\text{H}}$  (CDCl<sub>3</sub>) 7.20–7.60 (m, 15H, 3 × C<sub>6</sub>H<sub>5</sub>), 5.91 (s, 1H, OH), 4.70–5.05 (m, 6H, 3 × CH<sub>2</sub>Ph), 4.33–4.45 (m, 4H, 2 × OCH<sub>2</sub>CH<sub>3</sub>), 4.27 (d, 1H, H3,  $^3J_{3,4} = 2.8$  Hz), 4.16 (dd, 1H, H4  $^3J_{4,5} = 9.6$  Hz,  $^3J_{4,3} = 2.8$  Hz), 4.10 (m, 1H, H6), 3.79 (t, 1H, H5,  $^3J_{5,4} = ^3J_{5,6} = 9.6$  Hz), 1.47 (td, 3H, OCH<sub>2</sub>CH<sub>3</sub>,  $^3J_{\text{H,H}} = 7.0$  Hz,  $^4J_{\text{H,P}} = 0.6$  Hz), 1.43 (td, 6H, 2 × OCH<sub>2</sub>CH<sub>3</sub>,  $^3J_{\text{H,H}} = 7.0$  Hz,  $^4J_{\text{H,P}} = 0.6$  Hz), 1.39 (d, 3H, H7,  $^3J_{7,6} = 6.3$  Hz);  $\delta_{\text{C}}$ : 138.5–138.7 (3 × C, C<sub>6</sub>H<sub>5</sub>), 127.4–128.8 (15 × CH, C<sub>6</sub>H<sub>5</sub>), 96.4 (m, C, C2), 89.8 (m, CF<sub>2</sub>, C1), 81.1 (CH, C4), 79.7

(CH, C5), 75.6 (d, CH, C3,  $^3J_{\text{C,P}} = 5.5$  Hz), 75.4 (CH<sub>2</sub>, CH<sub>2</sub>Ph), 74.9 (CH<sub>2</sub>, CH<sub>2</sub>Ph), 72.5 (CH<sub>2</sub>, CH<sub>2</sub>Ph), 69.4 (CH, C6), 65.6 (d, CH<sub>2</sub>, OCH<sub>2</sub>,  $^2J_{\text{C,P}} = 6.2$  Hz), 17.7 (CH<sub>3</sub>, C7), 16.5 (d, CH<sub>2</sub>CH<sub>3</sub>,  $^3J_{\text{C,P}} = 6.1$  Hz);  $\delta_{\text{P}}$ : 8.17 (t, 1P,  $^2J_{\text{P,F}} = 96.9$  Hz);  $\delta_{\text{F}}$ : -117.36 to -119.00 (dd, 1F,  $^2J_{\text{F,F}} = 307.0$  Hz,  $^2J_{\text{F,P}} = 96.9$  Hz), -119.12 to -120.70 (dd, 1F,  $^2J_{\text{F,F}} = 307.0$  Hz,  $^2J_{\text{F,P}} = 96.9$  Hz). HRMS (ESI<sup>-</sup>): found [M - H]<sup>-</sup> 619.2296. C<sub>32</sub>H<sub>38</sub>F<sub>2</sub>O<sub>8</sub>P<sub>1</sub> requires [M - H]<sup>-</sup> 619.2278.

**Diethyl (3,4,5-Tri-*O*-benzyl-1-deoxy-1,1-difluoro-2-*O*-methyloxalyl- $\alpha$ -*L*-rhamno-heptulopyranosyl)phosphonate (16).** Diethyl (tri-*O*-benzyl-1-deoxy-*L*-rhamno-heptulopyranosyl)-1-difluorophosphonate (**14**) (0.149 g, 0.24 mmol) was dissolved in a mixture of 7:2 CH<sub>2</sub>Cl<sub>2</sub>:pyridine (5 mL), and methyl oxalyl chloride (MeOXCl) (0.2 mL, 2.1 mmol) was added to the mixture dropwise with stirring under nitrogen. After 90 min, TLC analysis showed complete consumption of **14** so the reaction was quenched with EtOH (0.5 mL) and was allowed to stir for 10 min before CH<sub>2</sub>Cl<sub>2</sub> (13 mL) and NaHCO<sub>3</sub> (5 mL, sat.) were added. The mixture was stirred for an additional 5 min after which it was poured into NaHCO<sub>3</sub> (10 mL, sat.) and extracted with CH<sub>2</sub>Cl<sub>2</sub> (3 × 15 mL) before being dried (Na<sub>2</sub>SO<sub>4</sub>) and concentrated. The result material was purified using column chromatography (30:70 EtOAc/hexane) to afford the product as a clear viscous liquid (**16**) (0.101 g, 69% yield):  $R_f = 0.64$  (50:50 EtOAc/hexane);  $\delta_{\text{H}}$  (CDCl<sub>3</sub>) 7.28–7.48 (m, 15H, 3 × C<sub>6</sub>H<sub>5</sub>), 5.37 (br s, OH, H3), 4.62–5.00 (m, 6H, 3 × CH<sub>2</sub>Ph), 4.21–4.43 (m, 4H, 2 × OCH<sub>2</sub>CH<sub>3</sub>), 4.07 (m, 1H, H6), 3.94 (s, 3H, OCH<sub>3</sub>), 3.86 (t, 1H, H5,  $^3J_{5,4} = ^3J_{5,6} = 9.4$  Hz), 3.72 (dd, 1H, H4  $^3J_{4,5} = 9.4$  Hz,  $^3J_{4,3} = 2.4$  Hz), 1.43 (d, 3H, H7,  $^3J_{7,6} = 6.2$  Hz), 1.47 (m, 6H, 2 × OCH<sub>2</sub>CH<sub>3</sub>);  $\delta_{\text{C}}$ : 157.1 (CO, C(O)C(O)OCH<sub>3</sub>), 154.5 (CO, C(O)C(O)OCH<sub>3</sub>), 137.6–138.6 (3 × C, C<sub>6</sub>H<sub>5</sub>), 127.5–128.8 (15 × CH, C<sub>6</sub>H<sub>5</sub>), 106.3 (m, CF<sub>2</sub>, C1) 80.0 (CH, C4), 78.9 (CH, C5), 75.8 (CH<sub>2</sub>, CH<sub>2</sub>Ph), 75.3 (CH<sub>2</sub>, CH<sub>2</sub>Ph), 73.0 (CH, C3), 72.3 (CH<sub>2</sub>, CH<sub>2</sub>Ph), 72.1 (CH, H6), 65.5 (d, CH<sub>2</sub>, OCH<sub>2</sub>,  $^2J_{\text{C,P}} = 6.3$  Hz), 65.2 (d, CH<sub>2</sub>, OCH<sub>2</sub>,  $^2J_{\text{C,P}} = 6.3$  Hz), 54.0 (CH<sub>3</sub>, OCH<sub>3</sub>), 17.9 (CH<sub>3</sub>, C7), 16.5 (m, CH<sub>2</sub>CH<sub>3</sub>);  $\delta_{\text{P}}$ : 3.82 (dd, 1P,  $^2J_{\text{P,F}} = 104.9$  Hz,  $^2J_{\text{P,P}} = 91.3$  Hz);  $\delta_{\text{F}}$ : -109.6 to -111.22 (dd, 1F,  $^2J_{\text{F,F}} = 320.6$  Hz,  $^2J_{\text{F,P}} = 91.3$  Hz), -113.60 to -115.25 (dd, 1F,  $^2J_{\text{F,F}} = 320.6$  Hz,  $^2J_{\text{F,P}} = 104.9$  Hz). HRMS (ESI<sup>+</sup>): found [M + Na]<sup>+</sup> 729.2258. C<sub>35</sub>H<sub>41</sub>F<sub>2</sub>O<sub>11</sub>P<sub>1</sub> requires [M + Na]<sup>+</sup> 729.2247.

**Diethyl (2,6-Anhydro-3,4,5-tri-*O*-benzyl-1-deoxy-1,1-difluoro- $\beta$ -*L*-rhamno-heptulopyranosyl)phosphonate (17).** Diethyl (tri-*O*-benzyl-2-deoxy-methylxalyl-*L*-rhamno-heptulopyranosyl)-1-difluorophosphonate (**16**) (0.100 g, 0.140 mmol) was dissolved in toluene (7 mL) and transferred to a three-neck round-bottom flask that had been degassed for 10 min. Tributyltin hydride (Bu<sub>3</sub>SnH) (87  $\mu$ L, 0.33 mmol) was added followed by dropwise addition of azobisisobutyronitrile (AIBN) (20 mol %, 0.14 mL, 0.028 mmol) over 1 min. The reaction was heated to 105 °C and stirred for 1 h. The reaction mixture was then cooled to room temperature and diluted with EtOAc (7 mL) followed by concentration. The resulting material was purified using column chromatography (27:73 EtOAc/hexane) to afford the product as a clear viscous liquid (**17**) (0.076 g, 85% yield):  $R_f = 0.32$  (40:60 EtOAc/hexane);  $\delta_{\text{H}}$  (CDCl<sub>3</sub>) 7.25–7.50 (m, 15H, 3 × C<sub>6</sub>H<sub>5</sub>), 4.60–5.00 (m, 6H, 3 × CH<sub>2</sub>Ph), 4.20–4.40 (m, 5H, H3, 2 × OCH<sub>2</sub>CH<sub>3</sub>), 3.91 (m, 1H, H2), 3.75 (t, 1H, H5,  $^3J_{5,4} = ^3J_{5,6} = 9.4$  Hz), 3.54 (dd, 1H, H4  $^3J_{4,5} = 9.5$  Hz,  $^3J_{4,3} = 2.7$  Hz), 3.50 (m, 1H, H6), 1.30–1.45 (m, 9H, H7, 2 × OCH<sub>2</sub>CH<sub>3</sub>);  $\delta_{\text{C}}$ : 138.2–138.6 (3 × C, C<sub>6</sub>H<sub>5</sub>), 127.6–128.8 (15 × CH, C<sub>6</sub>H<sub>5</sub>), 84.0 (CH, C4), 80.0 (CH, C5), 77.2 (CH, C6), 75.7 (CH, CH<sub>2</sub>, C2, CH<sub>2</sub>Ph), 74.6 (CH<sub>2</sub>, CH<sub>2</sub>Ph), 72.7 (CH, C3,  $^3J_{\text{C,P}} = 5.9$  Hz), 72.4 (CH<sub>2</sub>, CH<sub>2</sub>Ph), 64.9 (t, CH<sub>2</sub>, OCH<sub>2</sub>,  $^2J_{\text{C,P}} = 7.4$  Hz), 17.7 (CH<sub>3</sub>, C7), 16.6 (d, CH<sub>2</sub>CH<sub>3</sub>,  $^3J_{\text{C,P}} = 4.9$  Hz);  $\delta_{\text{P}}$ : 6.20 (t, 1P,  $^2J_{\text{P,P}} = 108.0$  Hz);  $\delta_{\text{F}}$ : -115.27 to -117.01 (dd, 1F,  $^2J_{\text{F,F}} = 314.7$  Hz,  $^2J_{\text{F,P}} = 102.3$  Hz), -123.62 to -125.34 (dd, 1F,  $^2J_{\text{F,F}} = 314.7$  Hz,  $^2J_{\text{F,P}} = 102.3$  Hz). HRMS (ESI<sup>+</sup>): found [M + Na]<sup>+</sup> 627.2320. C<sub>32</sub>H<sub>39</sub>F<sub>2</sub>Na<sub>1</sub>O<sub>7</sub>P<sub>1</sub> requires [M + Na]<sup>+</sup> 627.2294.

**Representative Procedure for the Deprotection of Methyl Protected Analogues.** A solution of methyl protected compound **8a**, **10a**, or **12a** (50 mg), 10% palladium on carbon (20 mg, 0.02 mmol), ethyl acetate (3 mL), and methanol (3 mL) was degassed under vacuum and saturated with hydrogen gas (1 atm balloon). The reaction was stirred overnight before the catalyst was filtered, and the solution



was concentrated. The material was directly dissolved in 6 M aqueous HCl (5 mL) and refluxed for 3 h before being concentrated with methanol (3 × 5 mL) and titrated to pH 8 with aqueous NH<sub>4</sub>OH (0.2 M). Lyophilization provided compounds **9**, **11**, and **13** were obtained in quantitative yields as their diammonium salts.

**Representative Procedure for the Deprotection of Benzyl Protected Analogues.** A solution of benzyl protected compound **8b**, **10b**, or **12b** (50 mg), 10% palladium on carbon (20 mg, 0.02 mmol), ethyl acetate (3 mL), and methanol (3 mL) was degassed under vacuum and saturated with hydrogen gas (1 atm balloon). The reaction was stirred overnight before the catalyst was filtered, and the solution was concentrated to a colorless oil. The material was dissolved in water (2 mL) and titrated to pH 8 with aqueous NH<sub>4</sub>OH (0.2 M). Upon lyophilization, compounds **9**, **11**, and **13** were obtained in quantitative yields as their diammonium salts.

**Representative Procedure for the Deprotection of Ethyl Protected Analogues.** A solution of ethyl protected compound **14** or **17** (50 mg) was dissolved in dichloromethane (2 mL) and cooled to 0 °C in an ice bath before TMSI (55 equiv) was added dropwise with stirring. The ice bath was removed, and the reaction was allowed to stir at room temperature for 5 h before being quenched with methanol (4 mL) and concentrated. The crude mixture was dissolved in water (10 mL) and extracted with diethyl ether (8 × 10 mL). The aqueous layer was concentrated with methanol (3 × 10 mL) before being taken up in water (2 mL) and passed through an Amberlite cation exchange column (H<sup>+</sup> form). Acid fractions were pooled, concentrated, and titrated to pH 8 with aqueous NH<sub>4</sub>OH (0.2 M). Lyophilization provided compounds **15** and **18** were obtained in high yields (94–95%) as their diammonium salts.

**Ammonium-(1-deoxy-α-L-rhamno-heptulopyranosyl)-phosphonate (α-L-Rhamnose-1C-ketosephosphonate) (9).** δ<sub>H</sub>: (D<sub>2</sub>O) 3.86 (m, 1H, H4), 3.60–3.83 (m, 2H, H3, H6), 3.24 (m, 1H, H5), 1.70–2.00 (m, 2H, H1), 1.15 (d, 3H, H7, <sup>3</sup>J<sub>7,6</sub> = 6.2 Hz). δ<sub>C</sub>: 93.93 (s, C, C2), 68.22–72.87 (4s, 4 × CH, C3–6), 48.80 (s, CH<sub>2</sub>, C1) 16.80 (s, CH<sub>3</sub>, C7). δ<sub>P</sub>: 15.41 (s, 1P). HRMS (ESI<sup>-</sup>): found [M – H]<sup>-</sup> 257.0417. C<sub>7</sub>H<sub>14</sub>O<sub>8</sub>P<sub>1</sub> requires [M – H]<sup>-</sup> 257.0432.

**Ammonium-(2,6-anhydro-1-deoxy-β-L-rhamno-heptulopyranosyl)-phosphonate (β-L-Rhamnose-1C-phosphonate) (11).** δ<sub>H</sub>: (D<sub>2</sub>O) 3.80 (br d, 1H, H3, <sup>3</sup>J<sub>3,4</sub> = 3.3 Hz), 3.74 (m, 1H, H2), 3.50 (dd, 1H, H4, <sup>3</sup>J<sub>4,5</sub> = 9.1 Hz, <sup>3</sup>J<sub>4,3</sub> = 3.3 Hz), 3.30–3.15 (m, 2H, H5, H6), 1.95 (ddd, 2H, H1a, H1b, <sup>2</sup>J<sub>H,P</sub> = 18.2 Hz, <sup>3</sup>J<sub>1,2</sub> = 6.7 Hz, <sup>2</sup>J<sub>H,H</sub> = 1.42 Hz), 1.15 (d, 3H, H7, <sup>3</sup>J<sub>7,6</sub> = 6.0 Hz). δ<sub>C</sub>: 76.09–72.24 (3 × CH, C4–6), 73.76 (d, CH, C2, <sup>2</sup>J<sub>C,P</sub> = 11.1 Hz), 71.07 (d, CH, C3, <sup>3</sup>J<sub>C,P</sub> = 9.3 Hz), 29.75–28.68 (d, CH<sub>2</sub>, C1, <sup>1</sup>J<sub>C,P</sub> = 135.8 Hz), 16.98 (s, CH<sub>3</sub>, C7). δ<sub>P</sub>: 24.81 (s, 1P). HRMS (ESI<sup>-</sup>): found [M – H]<sup>-</sup> 241.0478. C<sub>7</sub>H<sub>14</sub>O<sub>7</sub>P<sub>1</sub> requires [M – H]<sup>-</sup> 241.0483.

**Ammonium-(1-deoxy-R-1-fluoro-α-L-rhamno-heptulopyranosyl)-phosphonate (α-L-Rhamnose-1CF-ketosephosphonate) (L-Rhamnose-1CF-ketosephosphonate) (13).** δ<sub>H</sub>: (D<sub>2</sub>O) 4.43 (dd, 1H, H1, <sup>2</sup>J<sub>H,F</sub> = 45.4 Hz, <sup>2</sup>J<sub>H,P</sub> = 4.2 Hz), 3.86 (m, 1H, H4), 3.70–3.78 (m, 2H, H3, H6), 3.27 (t, 1H, H5, <sup>3</sup>J<sub>5,4</sub> = <sup>3</sup>J<sub>5,6</sub> = 9.8 Hz), 1.16 (d, 3H, H7, <sup>3</sup>J<sub>7,6</sub> = 6.1 Hz). δ<sub>C</sub>: 86.28–87.64 (m, CH, C1), 72.61 (s, CH, C5), 70.56 (s, CH, C3), 70.09 (s, CH, C4), 68.31 (s, CH, C6), 16.93 (CH<sub>3</sub>, C7). δ<sub>P</sub>: 11.00 (d, 1P, <sup>2</sup>J<sub>P,F</sub> = 67.9 Hz). δ<sub>F</sub>: –213.80 (d, 1F, <sup>2</sup>J<sub>F,P</sub> = 68.7 Hz). HRMS (ESI<sup>-</sup>): found [M – H]<sup>-</sup> 275.0338. C<sub>7</sub>H<sub>13</sub>F<sub>1</sub>O<sub>8</sub>P<sub>1</sub> requires [M – H]<sup>-</sup> 275.0338.

**Ammonium-(2,6-anhydro-1-deoxy-1,1-difluoro-β-L-rhamno-heptulopyranosyl)phosphonate (β-L-Rhamnose-1CF<sub>2</sub>-phosphonate) (L-Rhamnose-1CF<sub>2</sub>-ketosephosphonate) (15).** δ<sub>H</sub>: (D<sub>2</sub>O) 4.09 (d, 1H, H3, <sup>3</sup>J<sub>3,4</sub> = 3.6 Hz), 3.79 (dd, 1H, H4, <sup>3</sup>J<sub>4,5</sub> = 10.2 Hz, <sup>3</sup>J<sub>4,3</sub> = 3.6 Hz), 3.75 (m, 1H, H6) 3.31 (t, 1H, H5, <sup>3</sup>J<sub>5,4</sub> = <sup>3</sup>J<sub>5,6</sub> = 9.7 Hz), 1.20 (d, 3H, H7, <sup>3</sup>J<sub>7,6</sub> = 6.3 Hz). δ<sub>C</sub>: 72.05 (s, CH, C5), 70.29 (s, CH, C3), 68.90–70.20 (2s, 2 × CH, C4, C6), 16.76 (s, CH<sub>3</sub>, C7). δ<sub>P</sub>: 3.92 (t, 1P, <sup>2</sup>J<sub>P,F</sub> = 77.2 Hz). δ<sub>F</sub>: –116.84 to –118.43 (dd, 1F, <sup>2</sup>J<sub>F,F</sub> = 295.4 Hz, <sup>2</sup>J<sub>F,P</sub> = 77.2 Hz), –122.08 to –123.62 (dd, 1F, <sup>2</sup>J<sub>F,F</sub> = 295.4 Hz, <sup>2</sup>J<sub>F,P</sub> = 77.2 Hz). HRMS (ESI<sup>-</sup>): found [M – H]<sup>-</sup> 293.0240. C<sub>7</sub>H<sub>12</sub>F<sub>2</sub>O<sub>8</sub>P<sub>1</sub> requires [M – H]<sup>-</sup> 293.0243.

**Ammonium-(2,6-anhydro-1-deoxy-1,1-difluoro-β-L-rhamno-heptulopyranosyl)phosphonate (β-L-rhamnose-1CF<sub>2</sub>-phosphonate) (L-rhamnose-1CF<sub>2</sub>-phosphonate) (18).** δ<sub>H</sub>: (D<sub>2</sub>O) 4.41 (br d, 1H,

H3, <sup>3</sup>J<sub>1,2</sub> = 2.4 Hz), 3.80 (m, 1H, H2), 3.54 (dd, 1H, H4, <sup>3</sup>J<sub>4,5</sub> = 9.3 Hz, <sup>3</sup>J<sub>4,3</sub> = 3.4 Hz), 3.33 (m, 2H, H5, H6), 1.23 (d, 3H, H7, <sup>3</sup>J<sub>7,6</sub> = 5.7 Hz). δ<sub>C</sub>: 77.96 (s, CH, C2), 76.70 (s, CH, C6), 73.12 (s, CH, C4), 72.19 (s, CH, C5), 68.24 (s, CH, C3), 16.72 (s, CH<sub>3</sub>, C7). δ<sub>P</sub>: 3.08 (t, 1P, <sup>2</sup>J<sub>P,F</sub> = 89.2 Hz). δ<sub>F</sub>: –110.09 to –111.60 (dd, 1F, <sup>2</sup>J<sub>F,F</sub> = 297.1 Hz, <sup>2</sup>J<sub>F,P</sub> = 80.5 Hz), –119.76 to –121.22 (dd, 1F, <sup>2</sup>J<sub>F,F</sub> = 296.00 Hz, <sup>2</sup>J<sub>F,P</sub> = 78.3 Hz). HRMS (ESI<sup>-</sup>): found [M – H]<sup>-</sup> 277.0289. C<sub>7</sub>H<sub>12</sub>F<sub>2</sub>O<sub>7</sub>P<sub>1</sub> requires [M – H]<sup>-</sup> 277.0294.

## ■ ASSOCIATED CONTENT

### 📄 Supporting Information

NMR spectra, HPLC traces, kinetic parameter calculations, amino acid sequence alignments, Cps2L tolerance to DMSO, Michaelis–Menten and Lineweaver–Burk plots, and IC<sub>50</sub> curves. This material is available free of charge via the Internet at <http://pubs.acs.org>.

## ■ AUTHOR INFORMATION

### ✉ Corresponding Author

\*D. L. Jakeman. E-mail: david.jakeman@dal.ca.

### Notes

The authors declare no competing financial interest.

## ■ ACKNOWLEDGMENTS

RmlB-D (*Aneurinibacillus thermoaerophilis*) plasmids were provided by Dr. Joseph Lam, Department of Molecular and Cellular Biology, University of Guelph, Canada.<sup>41</sup> Human PNP plasmid was provided by Dr. Vern L. Schramm, Department of Biochemistry, Albert Einstein College of Medicine, USA.<sup>42</sup> This work was supported in part by the Natural and Engineering Sciences Council of Canada and the Canadian Institutes of Health Research.

## ■ REFERENCES

- Pallares, R.; Viladrich, P. F.; Linares, J.; Cabellos, C.; Gudiol, F. *Microb. Drug Resist. (New Rochelle, NY, U. S.)* **1998**, *4*, 339–347.
- Smith, A. M.; Klugman, K. P. *Antimicrob. Agents Chemother.* **1998**, *42*, 1329–1333.
- Grebe, T.; Hakenback, R. *Antimicrob. Agents Chemother.* **1996**, *40*, 829–834.
- Smith, A. M.; Klugman, K. P. *Antimicrob. Agents Chemother.* **1995**, *39*, 859–867.
- Markiewicz, Z.; Tomasz, A. *J. Clin. Microbiol.* **1989**, *27*, 405–410.
- Strateva, T.; Yordanov, D. *J. Med. Microbiol.* **2009**, *58*, 1133–1148.
- Qu, H.; Xin, Y.; Dong, X.; Ma, Y. *FEMS Microbiol. Lett.* **2007**, *275*, 237–243.
- Ma, Y.; Stern, R. J.; Scherman, M. S.; Vissa, V. D.; Yan, W.; Jones, V. C.; Zhang, F.; Franzblau, S. G.; Lewis, W. H.; McNeil, M. R. *Antimicrob. Agents Chemother.* **2001**, *45*, 1407–1416.
- Alphey, M. S.; Pirrie, L.; Torrie, L. S.; Boulkeroua, W. A.; Gardiner, M.; Sarkar, A.; Maringer, M.; Oehlmann, W.; Brenk, R.; Scherman, M. S.; McNeil, M.; Rejzek, M.; Field, R. A.; Singh, M.; Gray, D.; Westwood, N. J.; Naismith, J. H. *ACS Chem. Biol.* **2013**, *8*, 387–396.
- Barton, W. A.; Lesniak, J.; Biggins, J. B.; Jeffrey, P. D.; Jiang, J. Q.; Rajashankar, K. R.; Thorson, J. S.; Nikolov, D. B. *Nat. Struct. Biol.* **2001**, *8*, 545–551.
- Moretti, R.; Thorson, J. S. *J. Biol. Chem.* **2007**, *282*, 16942–16947.
- Zuccotti, S.; Zanardi, D.; Rosano, C.; Sturla, L.; Tonetti, M.; Bolognesi, M. *J. Mol. Biol.* **2001**, *313*, 831–843.
- Kornfeld, S.; Glaser, L. *J. Biol. Chem.* **1961**, *236*, 1791–1794.
- Blankenfeldt, W.; Asuncion, M.; Lam, J. S.; Naismith, J. H. *EMBO J.* **2000**, *19*, 6652–6663.
- Melo, A.; Glaser, L. *J. Biol. Chem.* **1965**, *240*, 398–405.

- (16) Engel, R. *Chem. Rev.* **1977**, *77*, 349–367.
- (17) Romanenko, V. D.; Kukhar, V. P. *Chem. Rev.* **2006**, *106*, 3868–3935.
- (18) Chang, W.; Dey, M.; Liu, P.; Mansoorabadi, S. O.; Moon, S.; Zhao, Z. K.; Drennan, C. L.; Liu, H. *Nature* **2013**, *496*, 114–118.
- (19) Cload, P. A.; Hutchinson, D. W. *Nucleic Acids Res.* **1983**, *11*, 5621–5628.
- (20) Fonong, T.; Burton, D. J.; Pietrzyk, D. J. *Anal. Chem.* **1983**, *55*, 1089–1094.
- (21) Chen, W.; Flavin, M. T.; Filler, R.; Xu, Z. *J. Chem. Soc., Perkin Trans.* **1998**, 3979–3988.
- (22) Hutchinson, D. W. *Antiviral Res.* **1985**, *5*, 193–205.
- (23) Blackburn, G. M. *Chem. Ind.* **1981**, 134–138.
- (24) Wnuk, S.; Robins, M. J. *Am. Chem. Soc.* **1996**, *118*, 2519–2520.
- (25) Nieschalk, J.; Batsanov, A.; OHagan, D.; Howard, J. *Tetrahedron.* **1996**, *52*, 165–176.
- (26) Berkowitz, D. B.; Bose, M.; Pfannenstiel, T. J.; Doukov, T. J. *Org. Chem.* **2000**, *65*, 4498–4508.
- (27) Forget, S. M.; Bhattasali, D.; Hart, V. C.; Cameron, T. S.; Syvitski, R. T.; Jakeman, D. L. *Chem. Sci.* **2012**, *3*, 1866–1878.
- (28) Fernández-Herrera, M. A.; Mohan, S.; López-Muñoz, H.; Hernández-Vázquez, J. M. V.; Pérez-Cervantes, E.; Escobar-Sánchez, M. L.; Sánchez-Sánchez, L.; Regla, I.; Pinto, B. M.; Sandoval-Ramírez, J. *Eur. J. Med. Chem.* **2010**, *45*, 4827–4837.
- (29) van Well, R. M.; Marinelli, L.; Erkelens, K.; van der Marel, G. A.; Lavecchia, A.; Overkleeft, H. S.; van Boom, J. H.; Kessler, H.; Overhand, M. *Eur. J. Med. Chem.* **2003**, 2303–2313.
- (30) Albright, J.; Goldman, L. J. *Am. Chem. Soc.* **1967**, *89*, 2416–2423.
- (31) Meyer, O.; Grosdemange-Billiard, C.; Tritsch, D.; Rohmer, M. *Org. Biomol. Chem.* **2003**, *1*, 4367–4372.
- (32) Norris, A. J.; Toyokuni, T. *J. Carbohydr. Chem.* **1999**, *18*, 1097–1105.
- (33) Nyffeler, P. T.; Duron, S. G.; Burkart, M. D.; Vincent, S. P.; Wong, C. H. *Angew. Chem., Int. Ed.* **2005**, *44*, 192–212.
- (34) Timmons, S. C.; Mosher, R. H.; Knowles, S. A.; Jakeman, D. L. *Org. Lett.* **2007**, *9*, 857–860.
- (35) Peng, J. W.; Moore, J.; Abdul-Manan, N. *Prog. Nucl. Magn. Reson. Spectrosc.* **2004**, *44*, 225–256.
- (36) Skinner, A. L.; Laurence, J. S. *J. Pharm. Sci.* **2008**, *97*, 4670–4695.
- (37) Beaton, S. A.; Huestis, M. P.; Sadeghi-Khomami, A.; Thomas, N. R.; Jakeman, D. L. *Chem. Commun.* **2009**, 238–240.
- (38) Timmons, S. C.; Hui, J. P.; Pearson, J. L.; Peltier, P.; Daniellou, R.; Nugier-Chauvin, C.; Soo, E. C.; Syvitski, R. T.; Ferrieres, V.; Jakeman, D. L. *Org. Lett.* **2008**, *10*, 161–163.
- (39) Cheng, Y. C.; Prusoff, W. H. *Biochem. Pharmacol.* **1973**, *22*, 3099–3108.
- (40) Webb, M. R. *Proc. Natl. Acad. Sci. U. S. A.* **1992**, *89*, 4884–4887.
- (41) Allard, S. T.; Giraud, M. F.; Whitfield, C.; Graninger, M.; Messner, P.; Naismith, J. H. *J. Mol. Biol.* **2001**, *307*, 283–295.
- (42) Lewandowicz, A.; Schramm, V. L. *Biochemistry* **2004**, *43*, 1458–1468.